Naphthoyl Benzhydrazine - Decorated Binuclear Arene Ru(II) Complexes as Anticancer Agents Targeting Human Breast Cancer Cells

Arunachalam Abirami,[a] Umapathy Devan,[b] Rengan Ramesh,[a*] Arockiam Antony Joseph Velanganni,[b] Jan Grzegorz Małecki [c]

[a]Centre for Organometallic Chemistry, School of Chemistry, Bharathidasan University, Tiruchirappalli – 620 024, India.

[b]Molecular Oncology Laboratory, Department of Biochemistry, School of Life Sciences, Bharathidasan University, Tiruchirappalli – 620 024, India.

[c]Department of Crystallography, Institute of Chemistry, University of Silesia, Katowice, Poland

[*]Corresponding author [Tel: +91-431-2407053, Fax: +91-431-2407045, E-mail: ramesh_bdu@yahoo.com]

TABLE OF CONTENTS

1. Materials, Methods and Crystal data collection

Commercially available $RuCl_3.3H_2O$ from LobaChemie was used. 1-Naphthoyl carbonyl chloride, 4-chloro, 4- methoxy, and unsubstituted benzhydrazideswere purchased from Sigma Aldrich. The starting materials $[(\eta^6\text{-benzene})RuCl_2]_2$and $[(\eta^6\text{-}p\text{-cymene})RuCl_2]_2$were prepared by literature methods.[1,2] Chemically pure and analar grade reagents were used for all the reactions. All the reagents used were chemically pure and analar grade. The solvents were freshly distilled before use by following standard procedures.[3]Boeties micro heating table was used to record the melting points and are uncorrected. The IR spectra of ligands and complexes were recorded within the range of 4000-400 cm^{-1} using Perkin-Elmer 597 spectrophotometer. A Cary 300 Bio UV–vis Varian spectrophotometer was utilized to record the electronic spectra of complexes in the range 800-200 nm. The ^{1}H-NMR spectra were recorded with Bruker 400 MHz instrument using TMS as internal reference in $CDCl_3$ and DMSO-d_6. A Micro mass thermo-scientific LTQ XL mass spectrometer was used for High-Resolution Mass Spectrometry of the complexes. Single crystals of complexes **1** and **6** were grown by slow evaporation of a dichloromethane and petroleum ether solution at room temperature. A single crystal of suitable size was covered with Paratone oil, mounted on the top of a glass fibre, and transferred to a Bruker AXS Kappa APEX II single crystal X-ray diffractometer using monochromated MoK_α radiation (λ = 0.71073). Data were collected at 293 K. The structure was solved by direct methods using SIR-97 and was refined by the full matrix least-squares method on F2 with SHELXL-97.[4,5] Non-hydrogen atoms were refined with anisotropy thermal parameters. All hydrogen atoms were geometrically fixed and collected to refine using a riding model. Complex**1** and **6** were drawn with ORTEP and the structural data have been deposited at the Cambridge Crystallographic Data Centre: CCDC for complex **1** and **6** are **2262242** and **2262243** respectively. Alert B has been observed and the reason has been given in the check cif.

2. Experimental Procedures

Stability studies

The Time-dependent UV-visible spectral method has been used to examine the stability of the complexes. Complexes were dissolved in a minimum amount of 1% DMSO and then diluted with PBS buffer to 1×10^{-3} M concentration. The summaries of hydrolysis of the complexes were monitored by electronic spectra over 72 h. [6]

Partition coefficient determination(log P)

The Hydrophobicity of the synthesized metal complexes **1-6** was determined to analyze the penetration behavior across the cell membrane. It is investigated in terms of partition coefficient (log P) using the "shake-flask" method between octanol/water phase partitions. Because of the substitution variation in different complexes, hydrophobicity differs. Octanol-saturated water (OSW) and water-saturated octanol (WSO) were prepared using analytical grade octanol (Sigma Aldrich) and doubly distilled water. Solubility and sample concentration play an important role in the measurements of given organic and aqueous medium compounds. Partition coefficients in a biphasic system were calculated by using the equation log P = log[(1−6)oct/(1−6)aq].[7] Complexes **1−6** (1 mg/mL; ethanol/water 1/6) were diluted to 2, 4, 6, 8, and 10 μg/mL in water; alternatively, these (1 mg/mL) were diluted to 2, 4, 6, 8, and 10 μg/mL in octanol, respectively. Required quantities of the complexes (4 mg/mL) were shaken for one day at room temperature in equal volume (50/50). Once it achieved equilibrium, two phases were separated and centrifuged. As a final point, each phase drug concentration was measured by UV-visible spectroscopy.

Cell culture

The human breast cancer cells (SkBr3, MCF-7, MDA-MB-468, MDA-MB-231) and non-cancerous cells (HEK-293 T- embryonic Kidney normal) were procured from the national center for cell science, Pune, India. The cells were maintained in DMEM medium with added 10% FBS (v/v) and 1% penicillin/streptomycin (w/v). The cultures were grown in 5% CO_2 and 95% humidified atmospheric conditions at 37˚C.

In vitro cytotoxicity using an MTT assay

The *in vitro* cytotoxicity of the complexes was measured by an MTT (3-(4,5-dimethylthiazol-2-yl)-2,5-diphenyltetrazolium bromide) assay. The cells were plated in flat-bottomed 96-well plates (4×10^3 cells per well) and incubated at 37 °C for 24 h. The cells were added via serial dilution of Complexes **1**-**6** and cisplatin and then incubated at 37 °C for 48 h. At the end of the exposure, 30 µL MTT solution (5 mg/mL in PBS) was added to each well. The MTT solution was removed from the wells after 4 h, and the purple MTT-formazan crystals were then dissolved by the addition of DMSO (100 µL). The absorbance in each well was measured at 490 nm using a microplate reader (Multiskan FC, ThermoScientific). DMSO blank assay has been performed before all cell assays.

Acridine orange-ethidium bromide (AO-EB) staining

4×10^3 of Sk-Br3cells were seeded in 24-well plates and incubated at 37 °C for 48 h. Complexes **1**-**6** (IC_{50} concentrations) were incubated with SkBr3 cells. After incubation, AO (100 µg/mL) and EB (100 µg/mL) were added to each well (500 µL). After 5 min, the cells were visualized via a fluorescence microscope (Olympus, BX-60, Japan), and the cell death was measured in three random fields of the microscope. Live cells were analysed by green filter(ex/em: 500/530nm) and dead cells were analysed by red filter(ex/em: 510/595nm)

Hoechst 33342 staining method

Hoechst 33342 staining was done using the method described earlier with slight modifications. 5×10^5SkBr3 cells were treated with IC_{50} concentration of the complexes **1-6** for 48 h in a 6-well culture plate and were fixed with 4% paraformaldehyde followed by permeabilization with 0.1% Triton X-100. Cells were then stained with 50 µg mL^{-1} Hoechst 33342 (ex/em: 357/540nm) for 30 min at room temperature. The cells undergoing apoptosis, represented by the morphological changes of apoptotic nuclei, were observed and imaged by an epifluorescence microscope (Carl Zeiss, Germany).

Reactive Oxygen Species (ROS) Assay

For quantifying the intracellular ROS, 5×10^5 SkBr3 cells were seeded on a 6-well plate containing a coverslip and incubated overnight for attachment. After incubation, the cells were treated with a fresh medium containing a lethal dose of complexes 1-6

and incubated further for 48 h. At the end of incubation, the coverslip was removed from the culture plate and stained with 40 μM of 2',7'-dichlorofluorescein-diacetate (DCFHDA: ex/em:495/529 nm) dye for 30 min. The stained coverslip was washed with PBS solution and visualized under fluorescence to record images.

Mitochondrial membrane potential(MMP)

The mitochondrial membrane potential of SkBr3 was assessed using the fluorescent dye Rhodamine 123. SkBr3 cells were cultured in a 6-well plate at $1x10^5$ cells/well density. Following treatment, the culture medium was carefully removed and cells were washed twice with PBS. The cells were subsequently stained with 2 μM Rhodamine 123 (ex/em:488/525 nm) for 20 min at 37°C in the dark. Cells were analyzed under a fluorescence microscope (20x, Floid cell imaging station, Life Technologies, USA).

Western blot

SkBr3cancer cells (3×10^5) were seeded into 6-well plates for 48 h and incubated with the complexes (25 μM) in the presence of 10 % FBS. Then, the cells were collected using trypsinization, washed 3 times with PBS, lysed in cell lysis buffer and 2 μg/mL leupeptin, and centrifuged at 10000 rpm for 10 min at 4 °C. The protein concentration of the supernatant was determined by bicinchoninic acid (BCA) assay. The samples were subjected to SDS-polyacrylamide gel electrophoresis (SDS-PAGE) with 10 % resolving gel. Gels were then exchanged by poly(vinylidenedifluoride) membranes (Millipore) and obstructed with 5 % non-fat milk in Tris-buffered saline (TBST, 0.1% Tween 20) buffer for 1 h. After the membranes were incubated with primary antibodies at 1:2000 dilutions in 5 % non-fat milk overnight at 37 °C, the membranes were washed 4 times with TBST buffer. Then, the secondary antibodies were conjugated with horseradish peroxidase at 1:2000 dilutions for 1 h at room temperature and afterward washed 4 times with TBST buffer. To evaluate the presence of a comparable quantity of proteins in every lane, the membranes were stripped finally to detect β-actin followed by visualization with the enhanced chemiluminescence (ECL) PLUS detection reagents following the manufacturer's procedure (Amersham Biosciences).

Annexin V-FITC/PI staining by flow cytometry method

Cells were seeded in a 6-well plate (10^5 cells/well)) and cultured at 37 °C for 48 h. The cells were then exposed to samples and incubated for 24 h. Next, the cells were incubated with IC50 concentration of the samples for 48 h. Then, the cells were trypsinized and washed with PBS. Next, the cells were stained with annexin V-FITC/PI(ex/em:488 nm/350 nm) according to the annexin V-FITC apoptosis detection kit. Finally, apoptosis was evaluated by a flow cytometer (SYSMEX, Japan), and the data were analyzed by Flow Jo software. The cells without any treatment were used as blank control.

3. UV-Vis spectra of ligands (NL1-NL3)

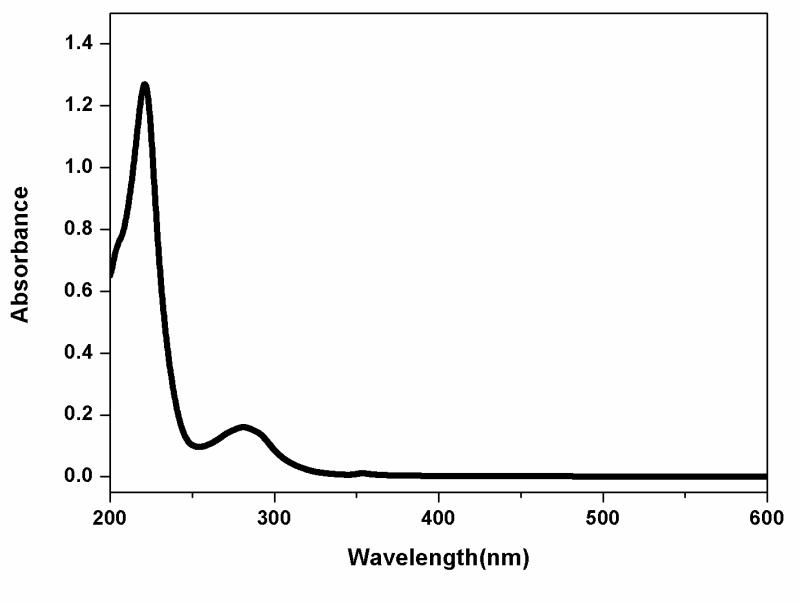

Figure S1. UV-Vis spectrum of Ligand NL1

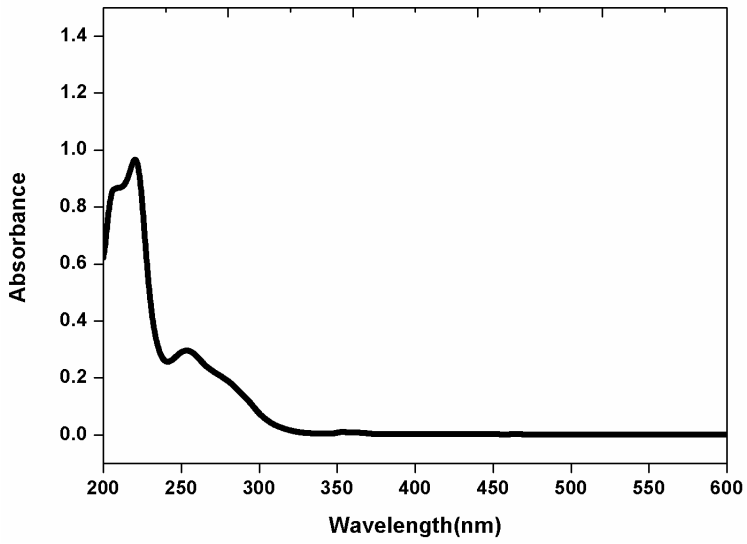

Figure S2. UV- Vis Spectrum of Ligand NL2

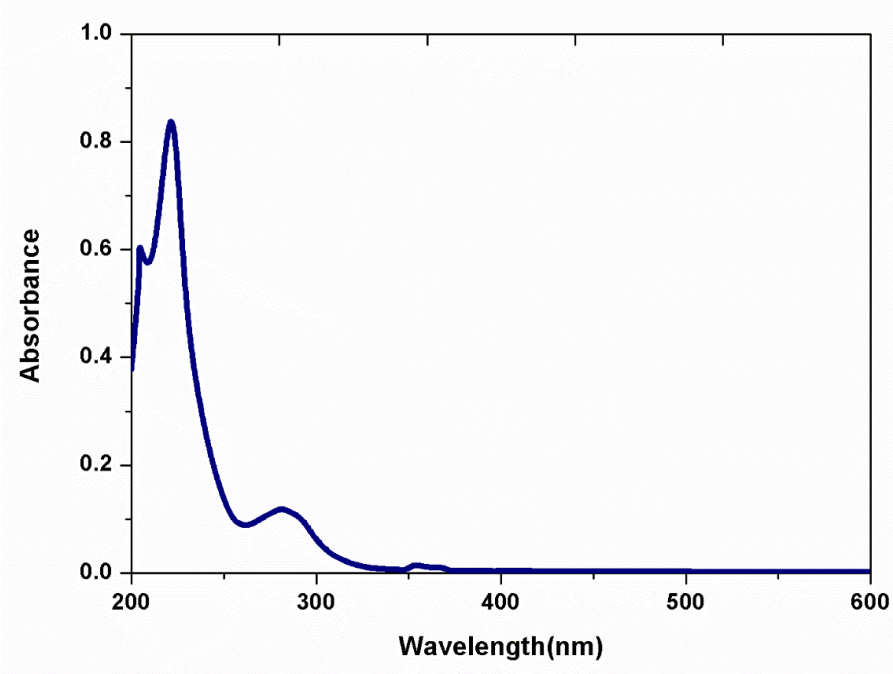

Figure S3. UV- Vis Spectrum of Ligand NL3

4. UV-Vis spectra of complexes (1-6)

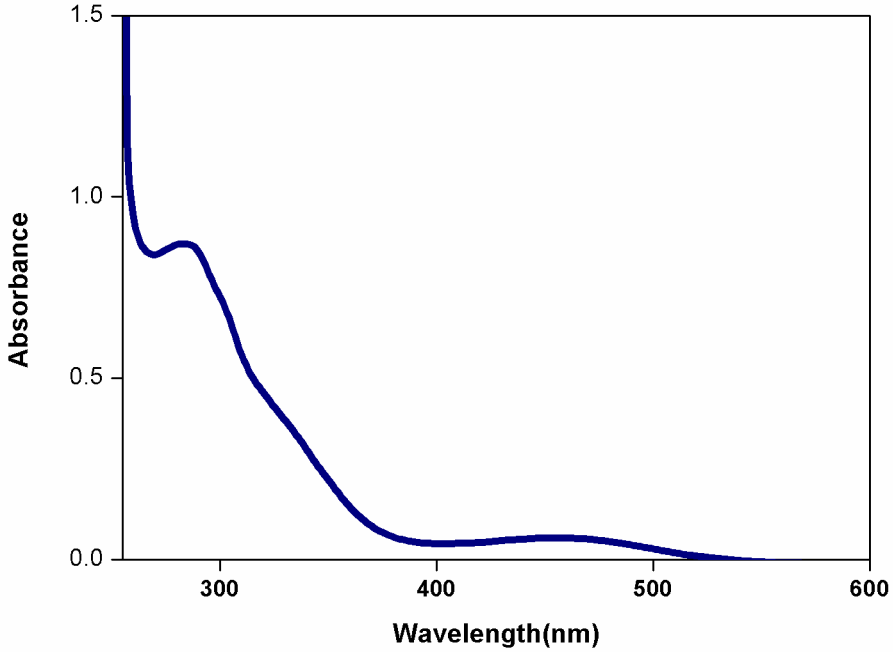

Figure S4. UV- Vis Spectrum of Complex **1**

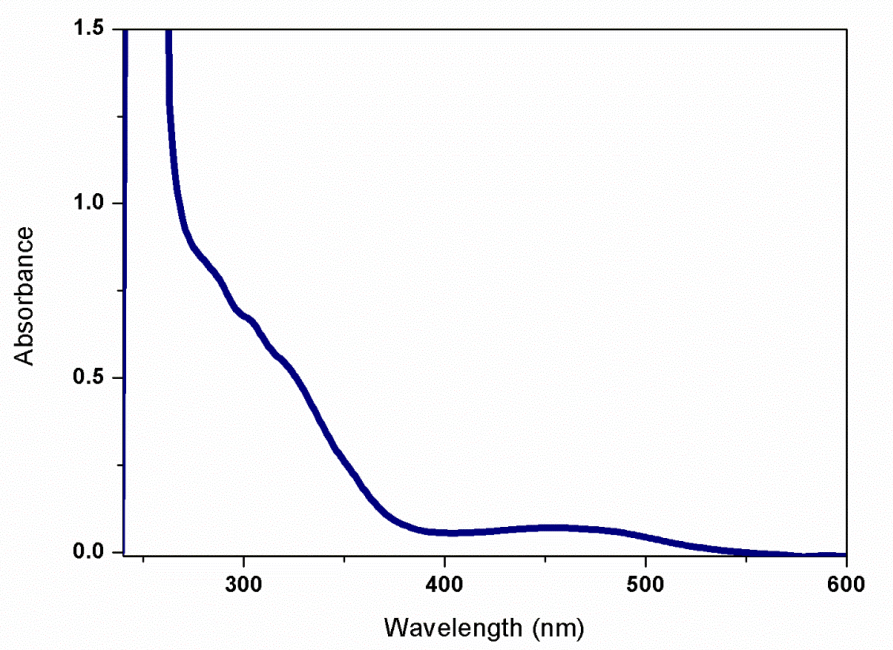

Figure S5. UV- Vis Spectrum of Complex **2**

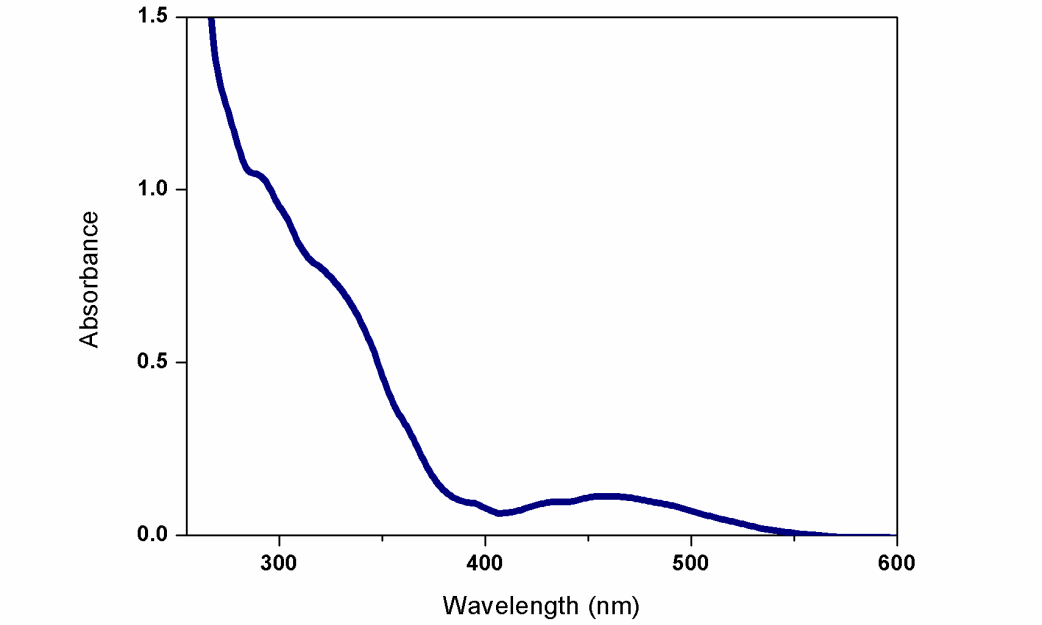

Figure S6. UV- Vis Spectrum of Complex **3**

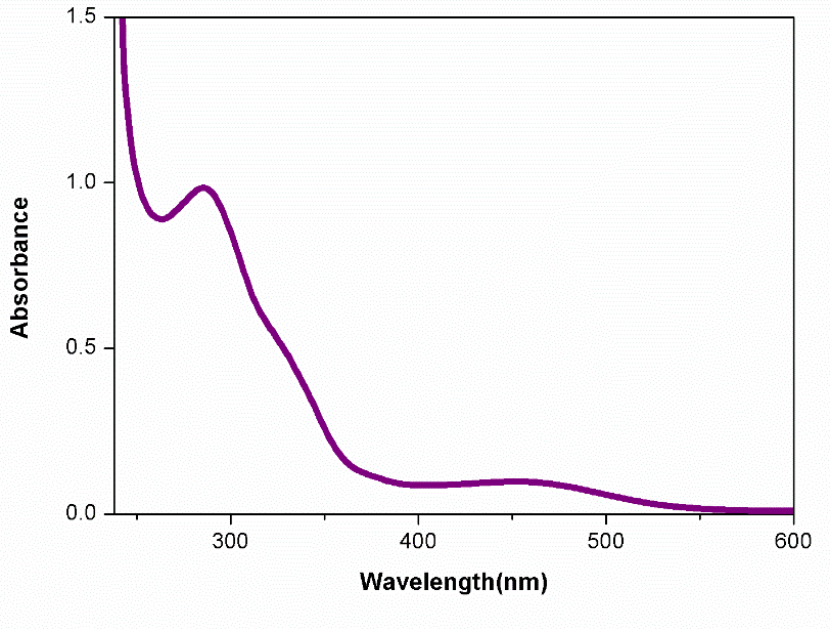

Figure S7. UV-Vis spectrum of complex **4**

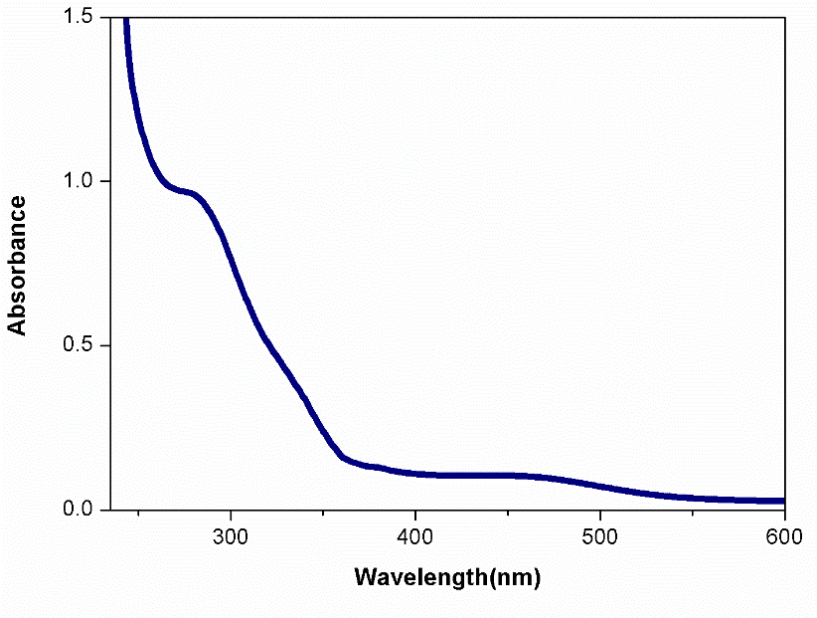

Figure S8. UV-Vis spectrum of complex **5**

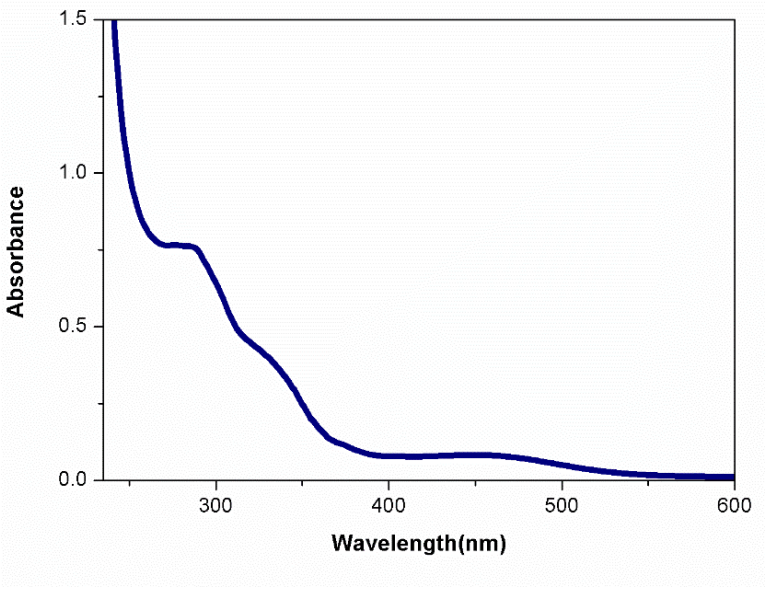

Figure S9. UV-Vis spectrum of complex **6**

5. ^{1}H and ^{13}C $\{^{1}H\}$NMR spectra of the ligands(1-3) and complexes(1-6)

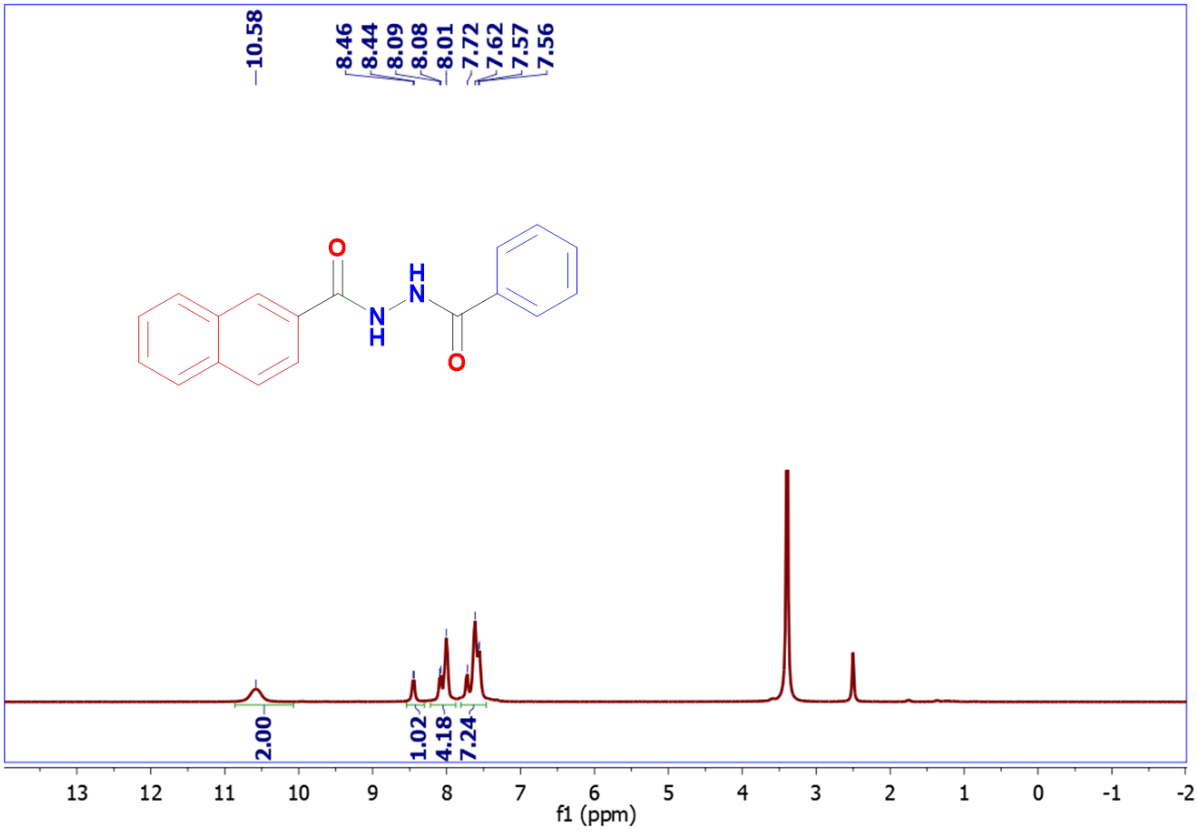

Figure S10. ^{1}H NMR spectrum of Ligand NL1

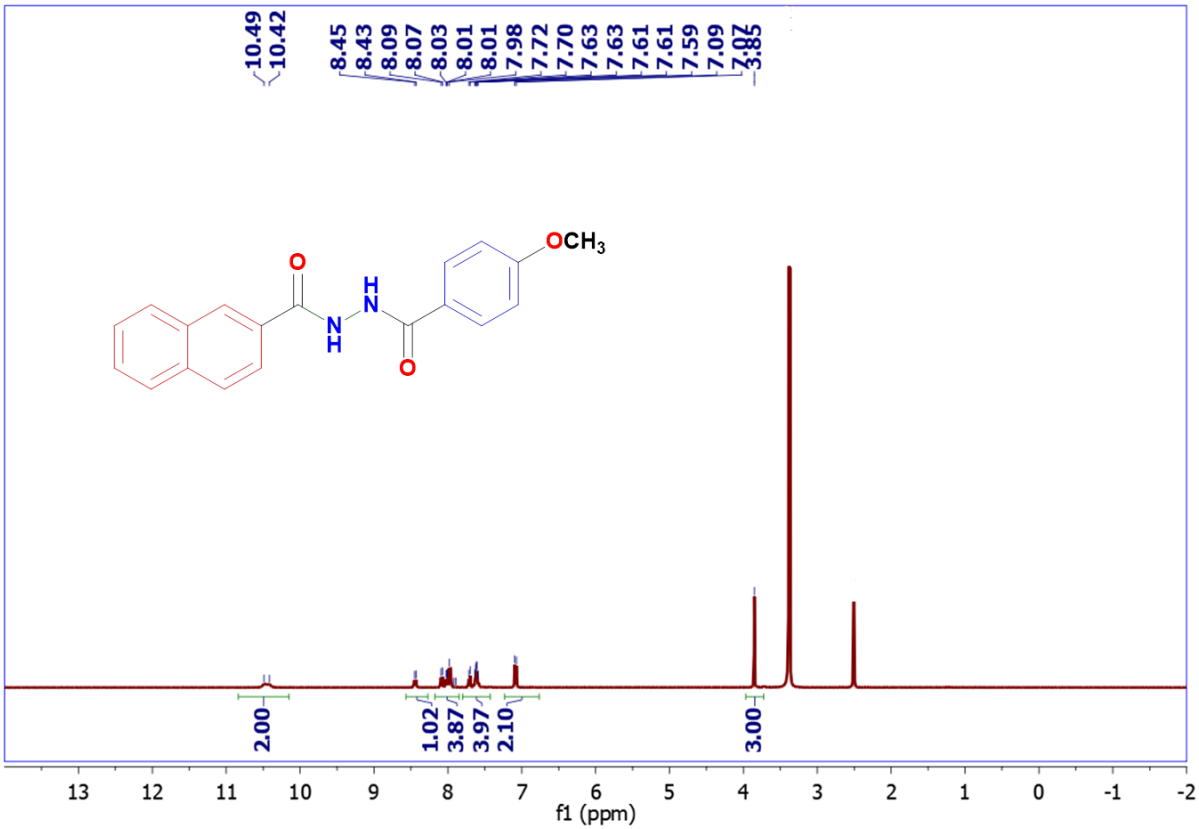

Figure S11.^{1}H NMR spectrum of Ligand NL2

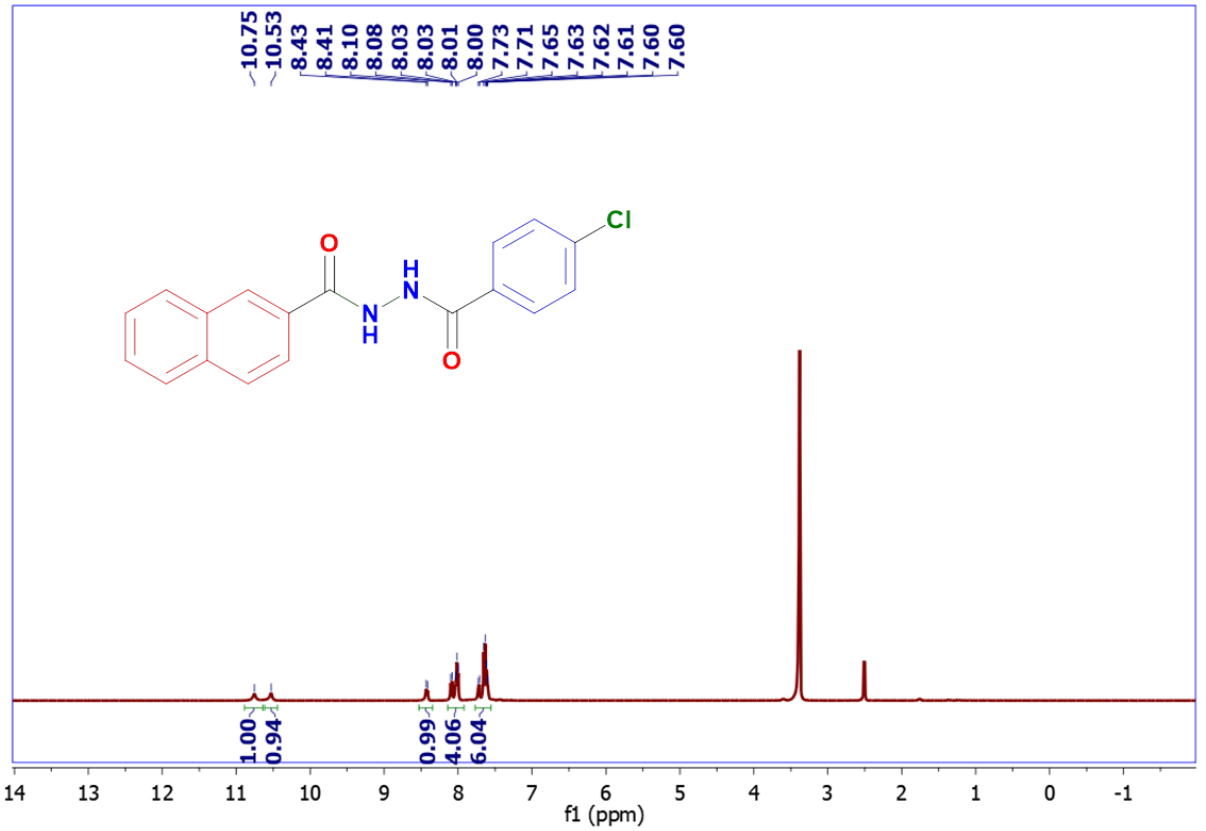

Figure S12.^{1}H NMR spectrum of Ligand NL3

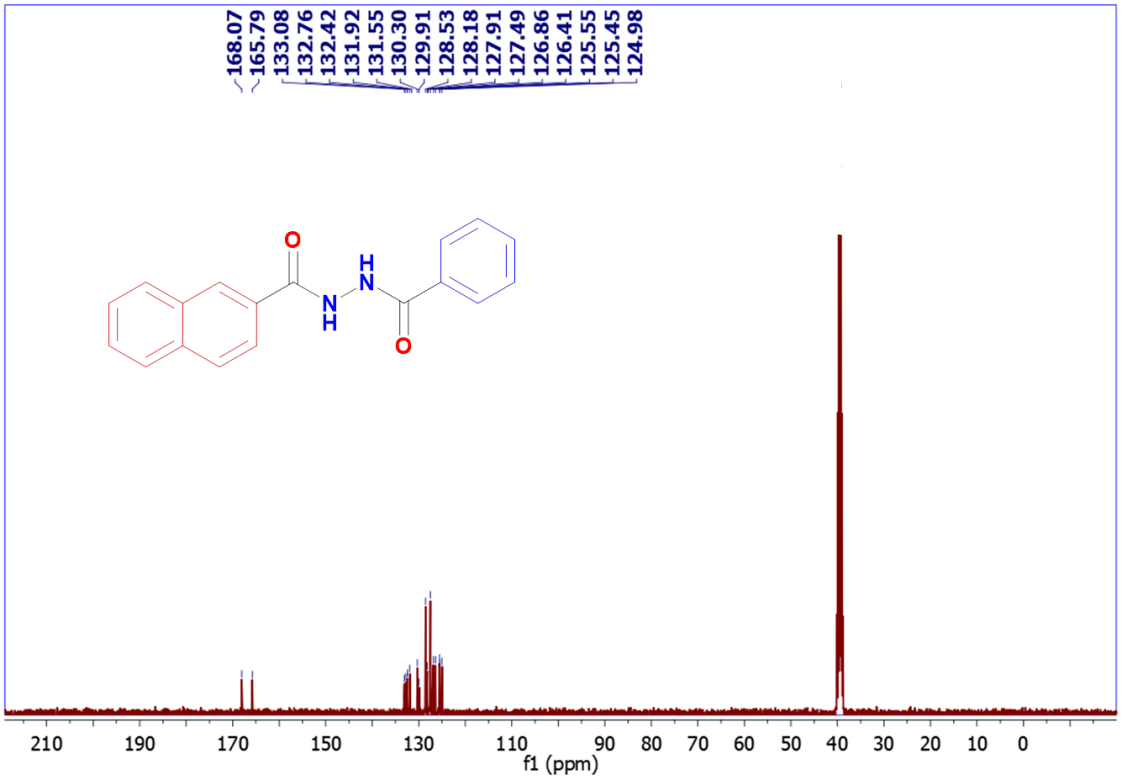

Figure S13. $^{13}C\{^{1}H\}$ NMR spectrum of Ligand NL1

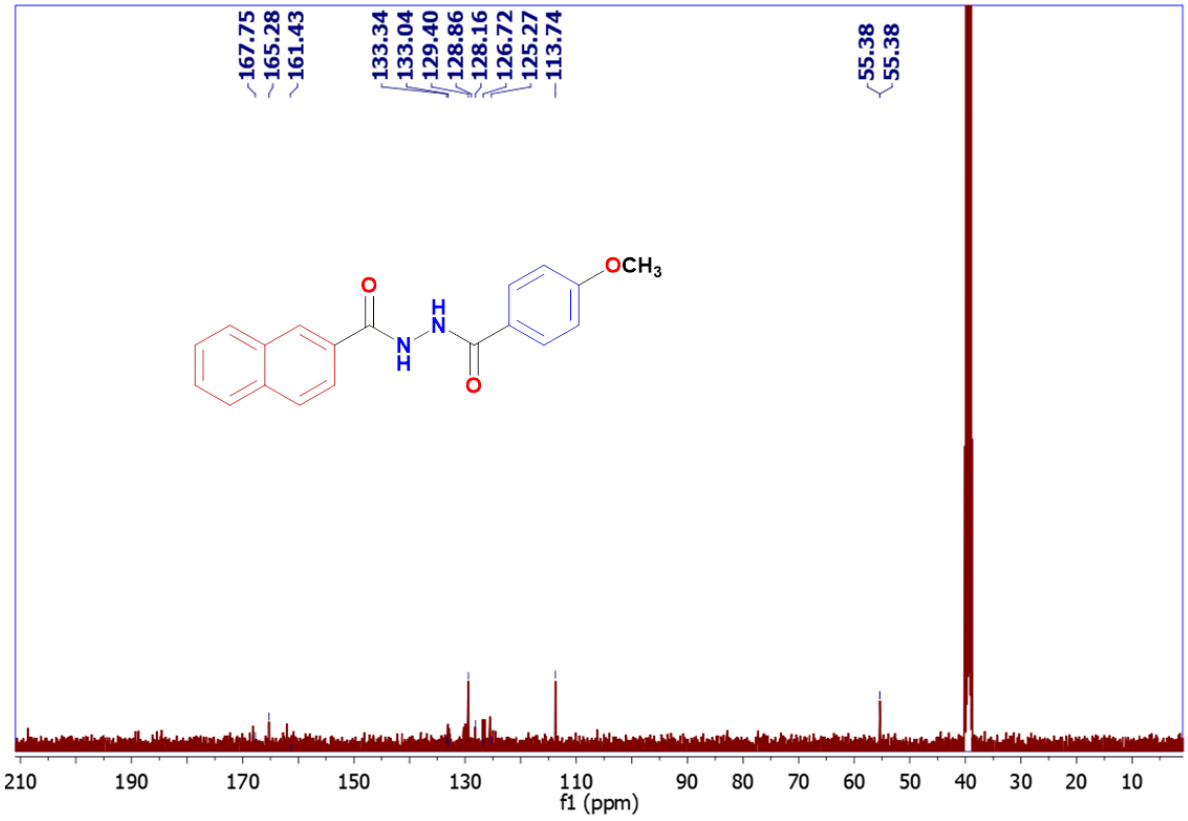

Figure S14. $^{13}C\{^{1}H\}$ NMR spectrum of Ligand NL2

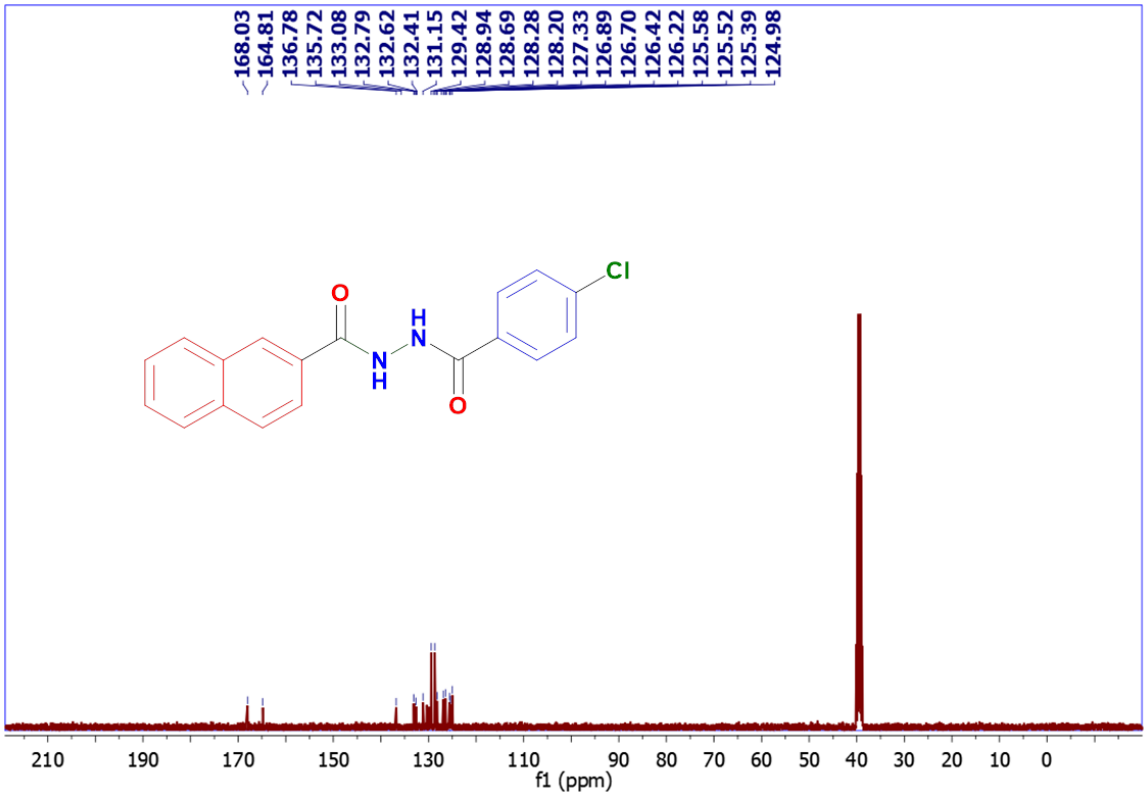

Figure S15. $^{13}C\{^{1}H\}$ NMR spectrum of Ligand NL3

6. ^{1}H and ^{13}C $\{^{1}H\}$NMR spectra of the complexes(1-6)

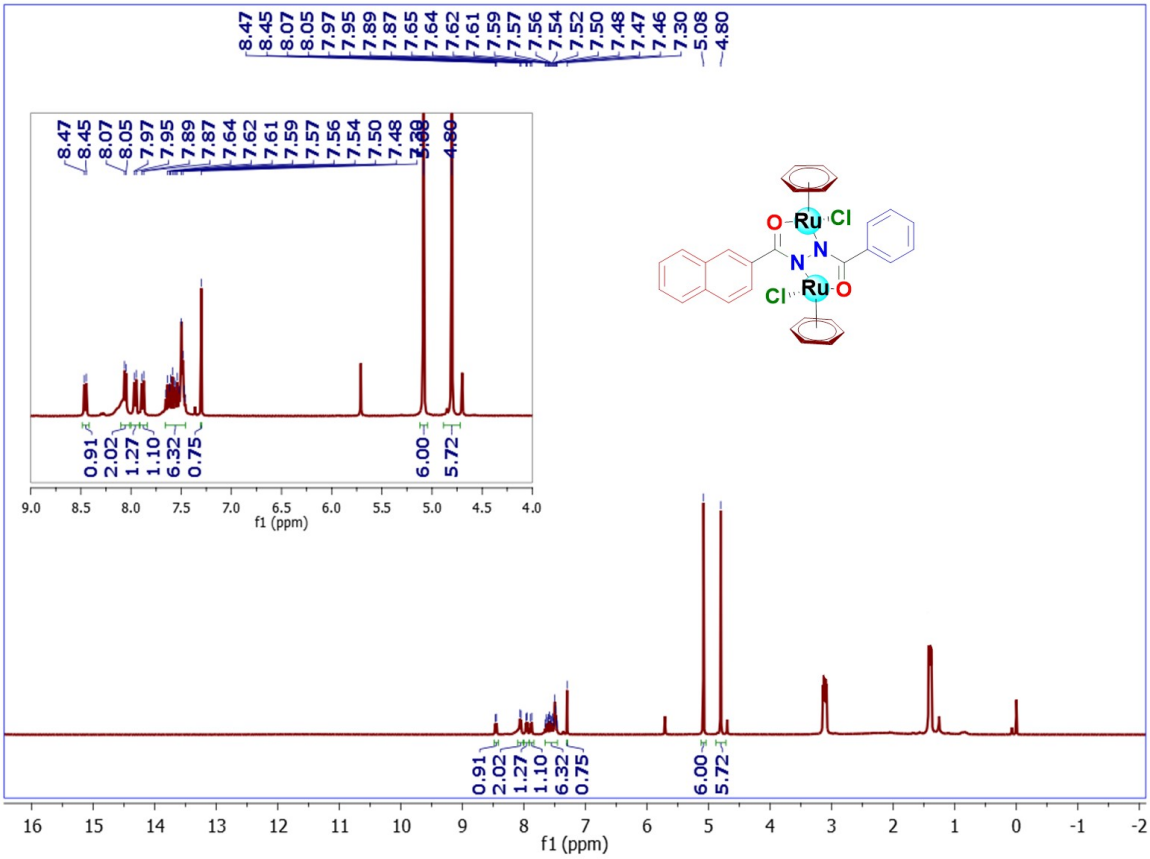

Figure S16. ^{1}H NMR spectrum of Complex **1**

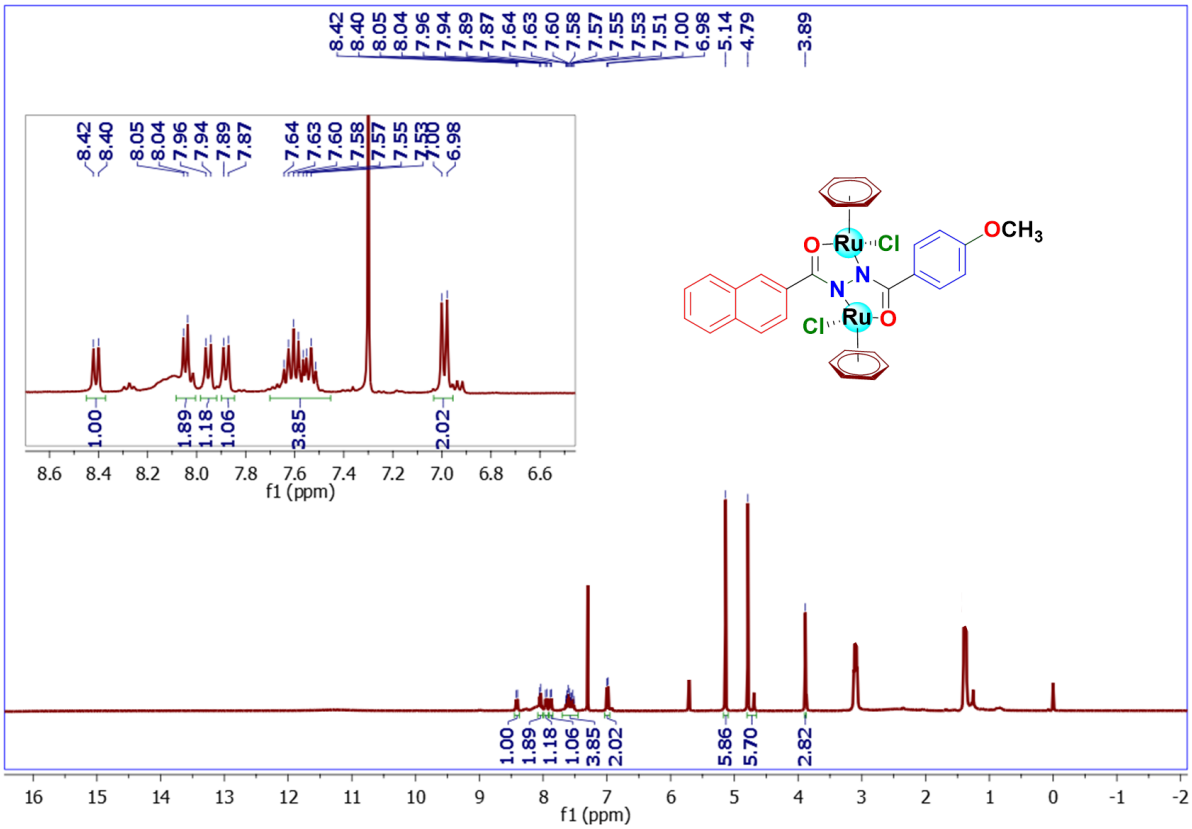

Figure S17. ^{1}H NMR spectrum of Complex **2**

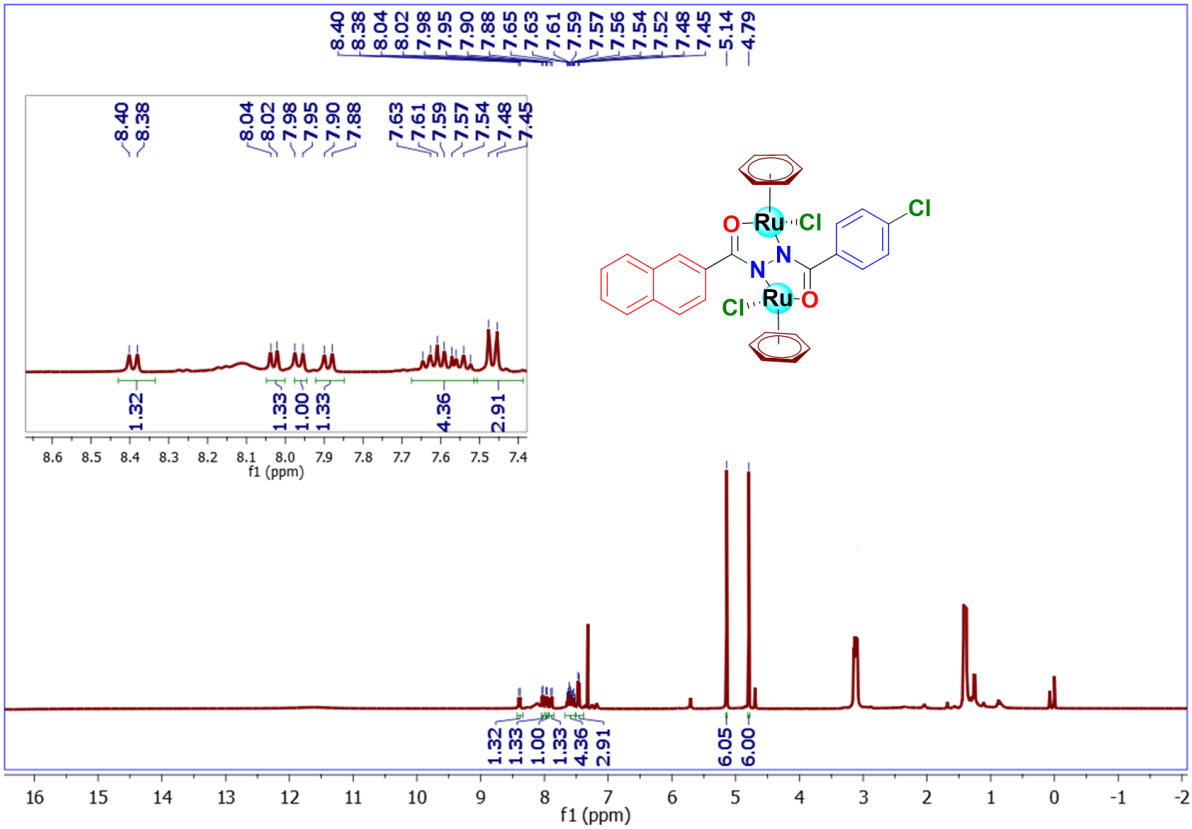

Figure S18. ^{1}H NMR spectrum of Complex **3**

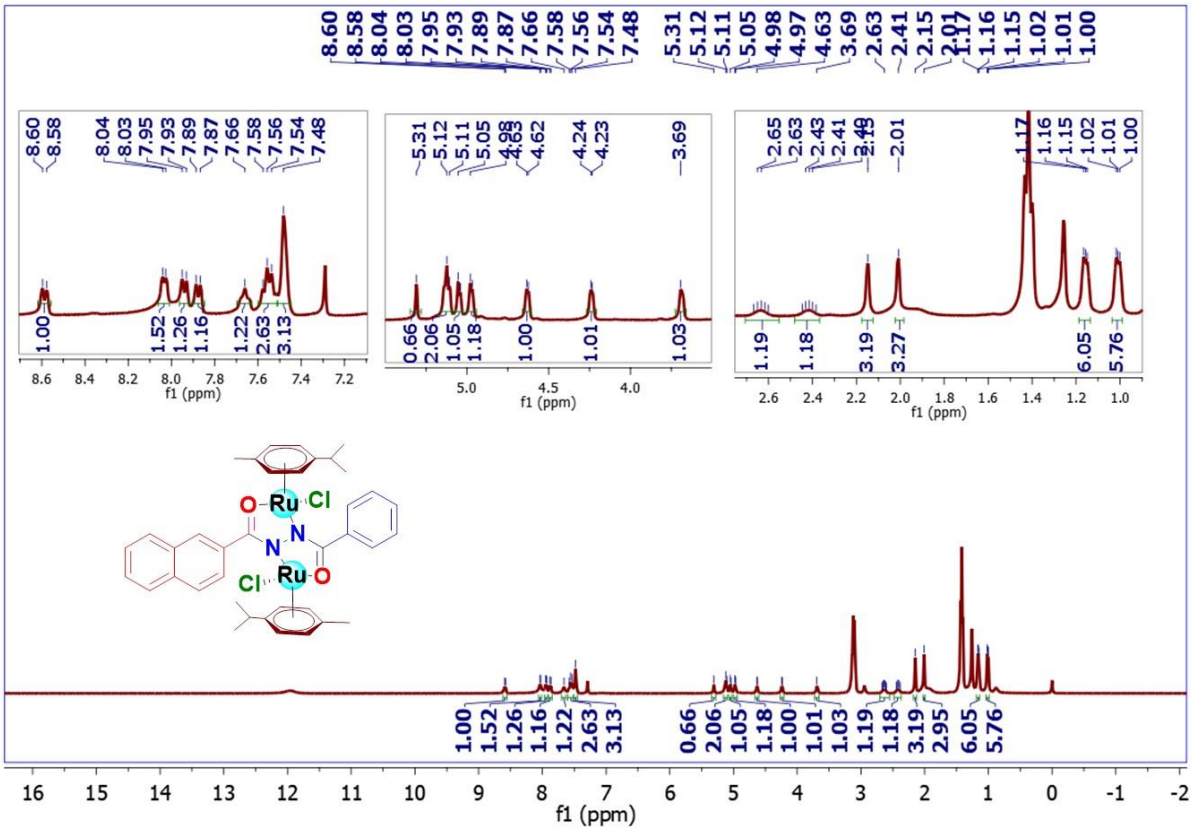

Figure S19. ^{1}H NMR spectrum of Complex **4**

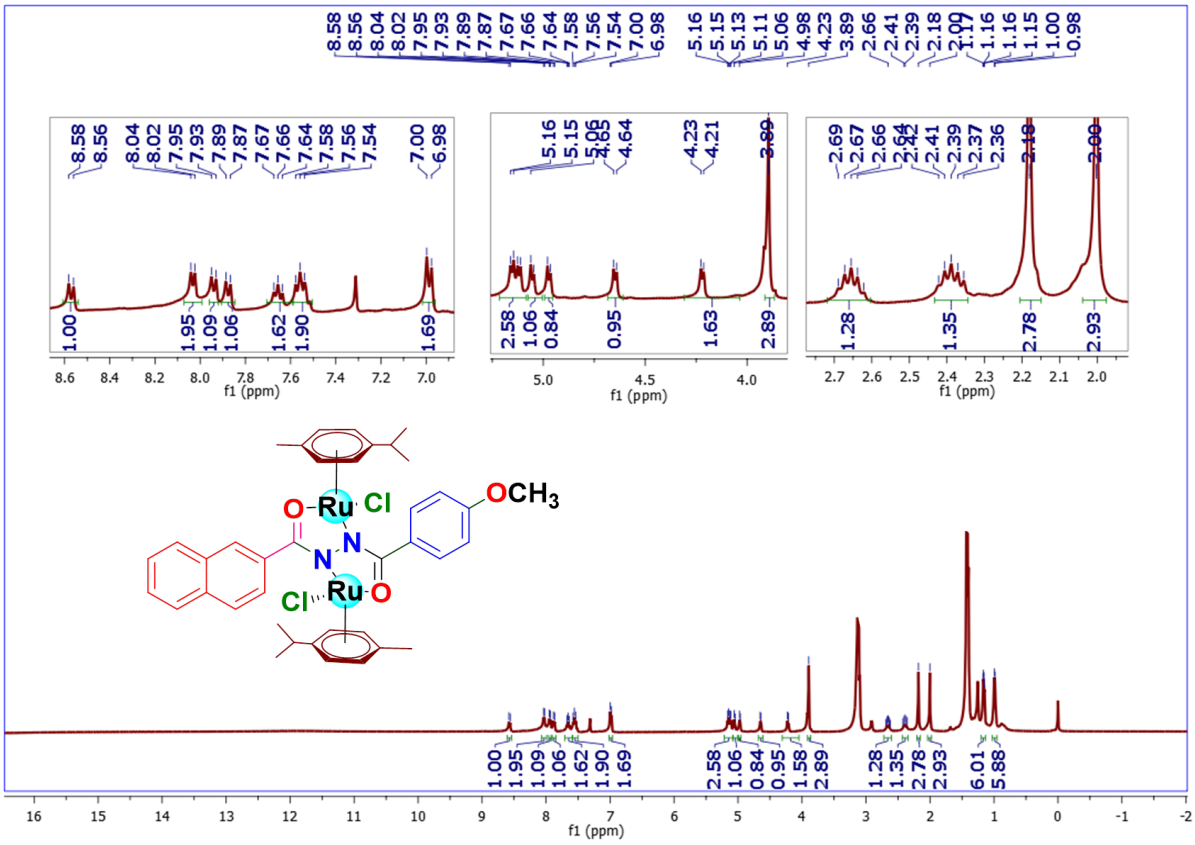

Figure S20. ^{1}H NMR spectrum of Complex **5**

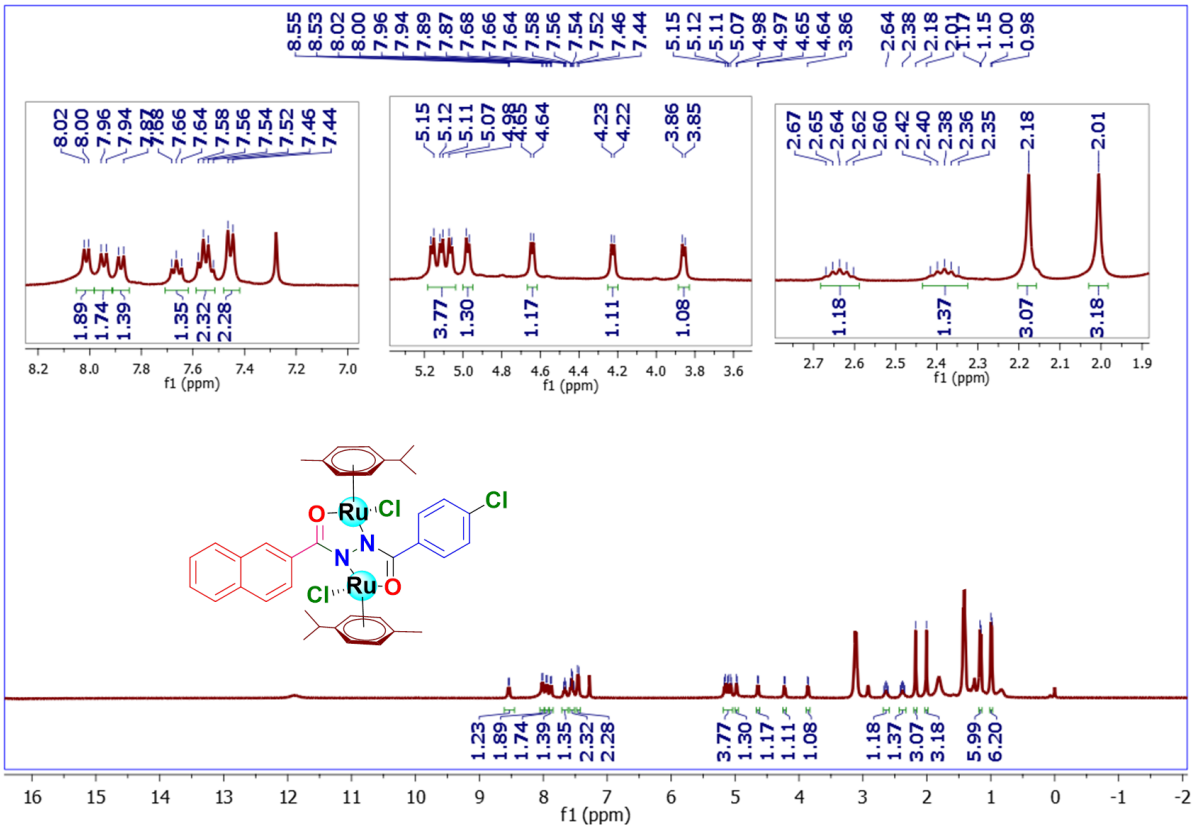

Figure S21. ^{1}H NMR spectrum of Complex **6**

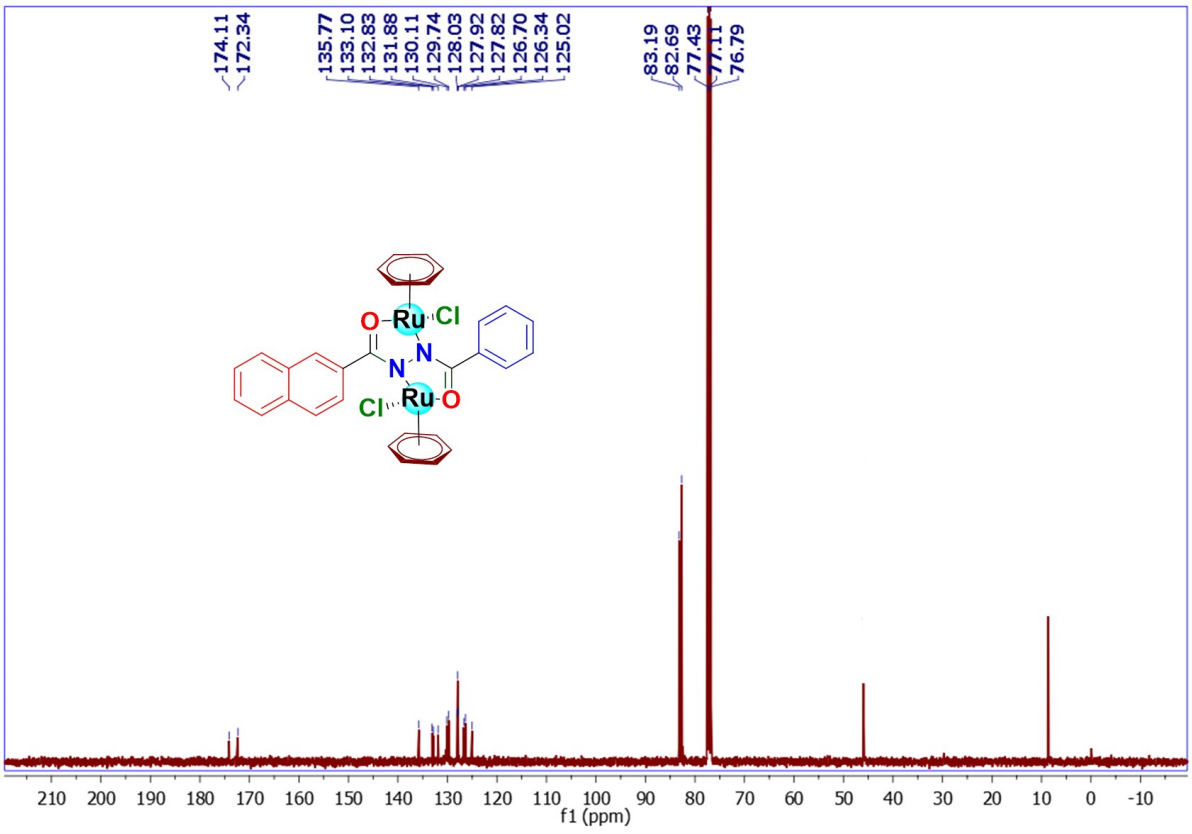

Figure S22. $^{13}C\{^{1}H\}$ NMR spectrum of Complex **1**

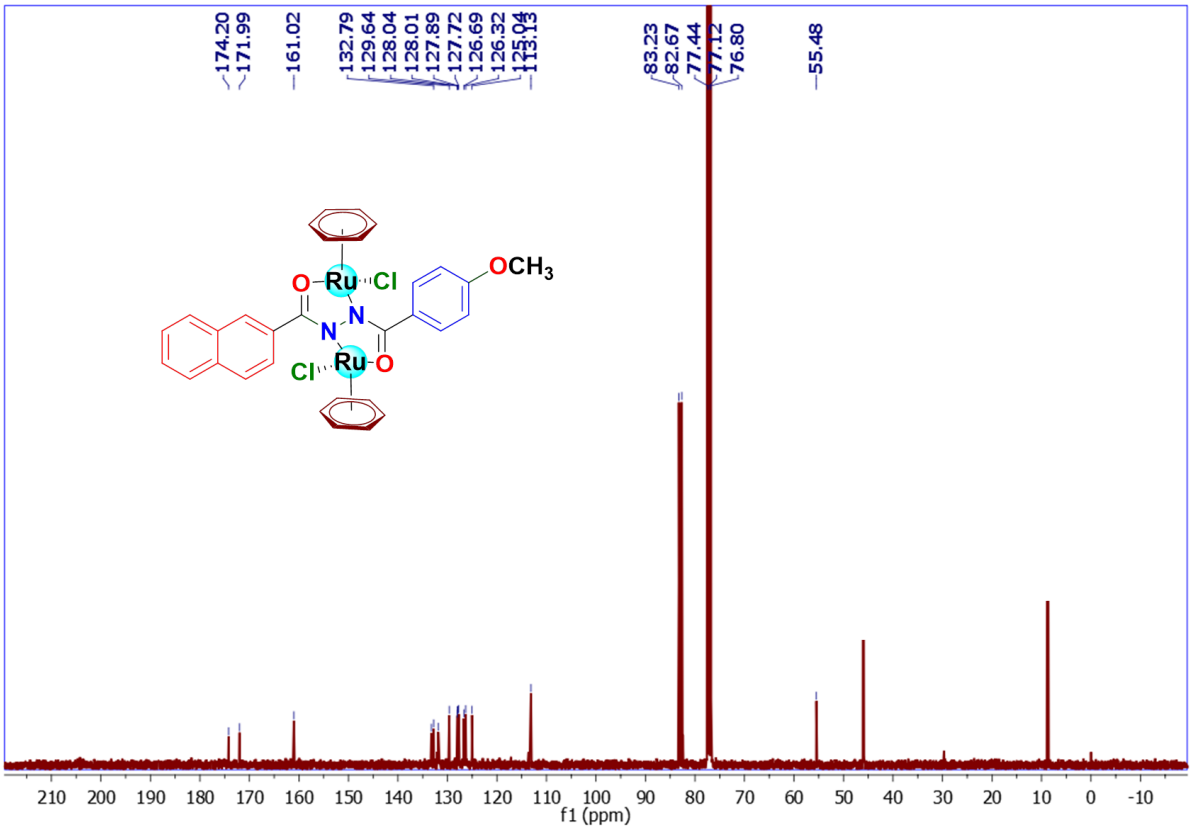

Figure S23. $^{13}C\{^{1}H\}$ NMR spectrum of Complex **2**

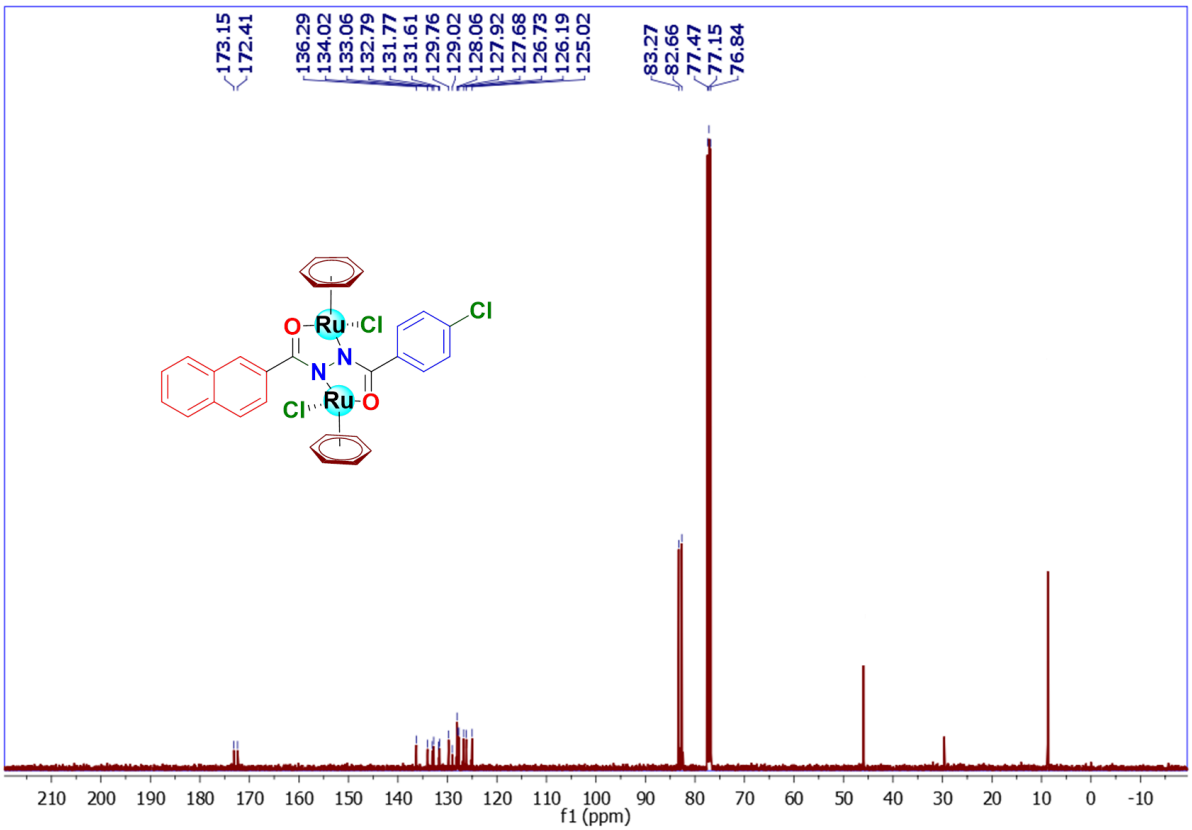

Figure S24. $^{13}C\{^{1}H\}$ NMR spectrum of Complex **3**

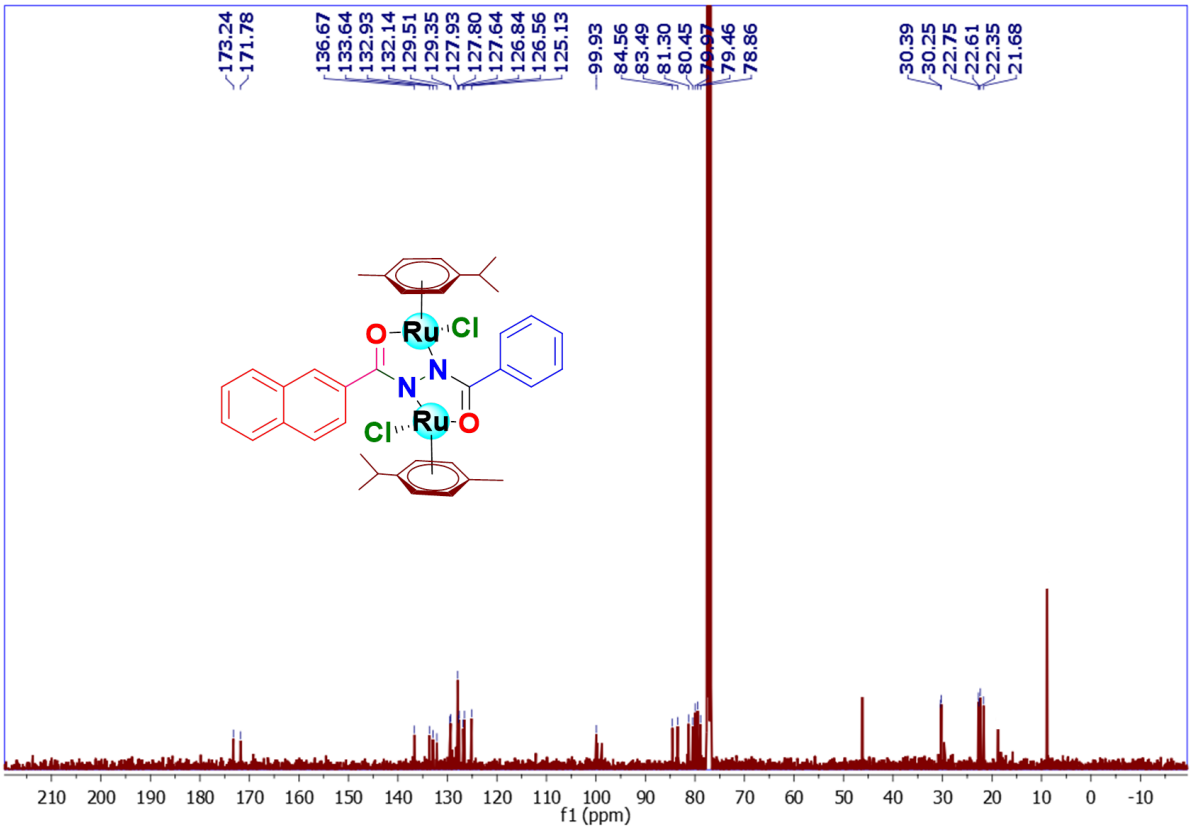

Figure S25. $^{13}C\{^{1}H\}$ NMR spectrum of Complex **4**

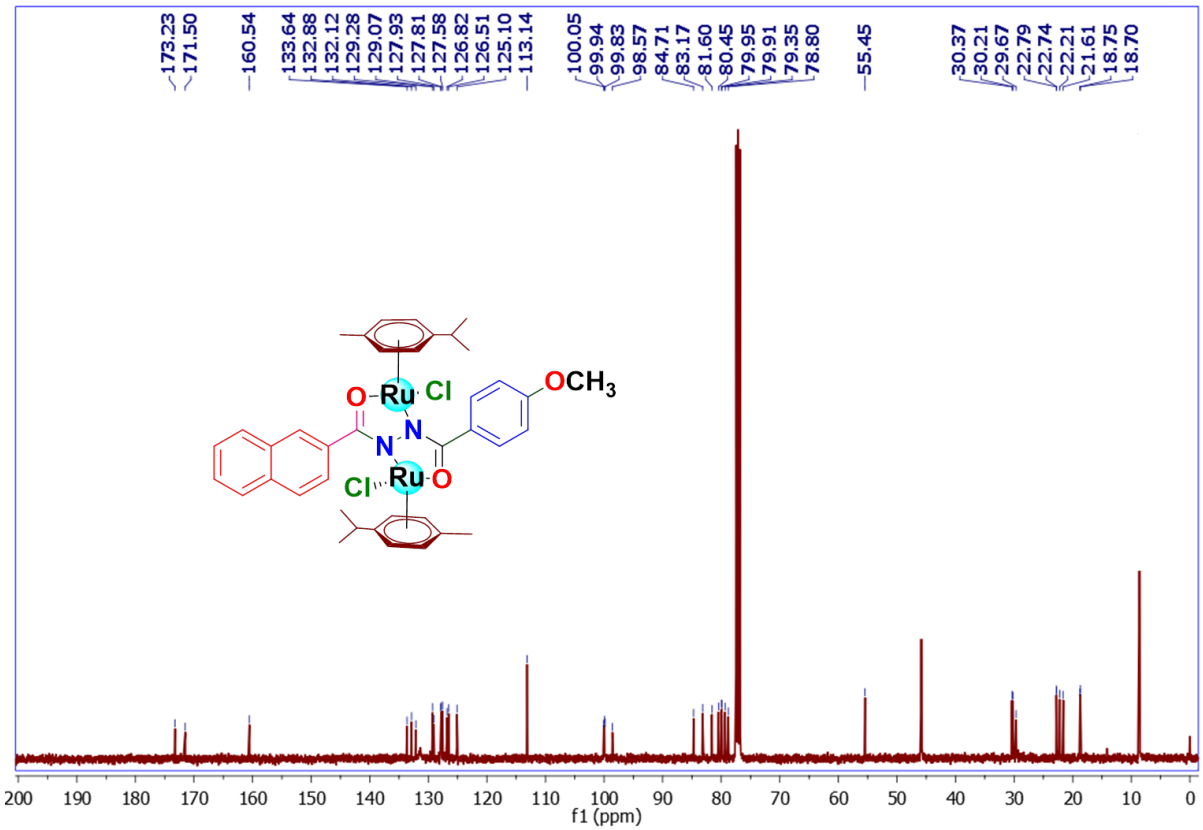

Figure S26. $^{13}C\{^{1}H\}$ NMR spectrum of Complex **5**

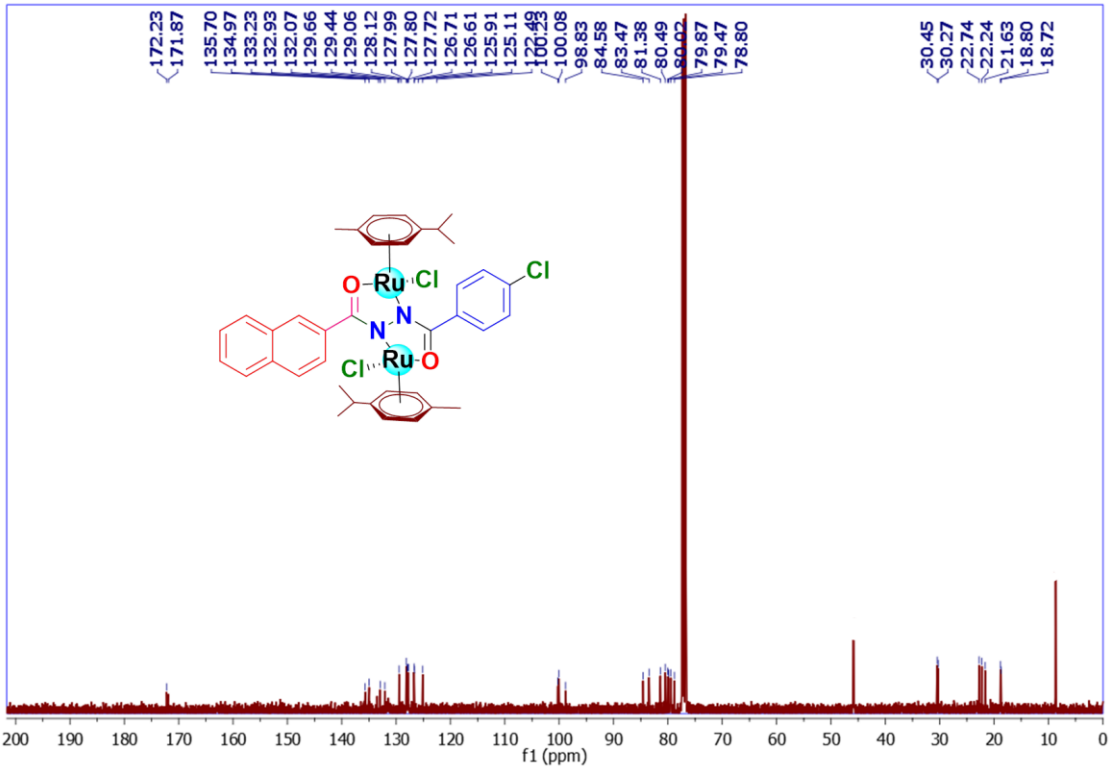

Figure S27. $^{13}C\{^{1}H\}$ NMR spectrum of Complex **6**

7. HR-MS spectra of the complexes(1-6)

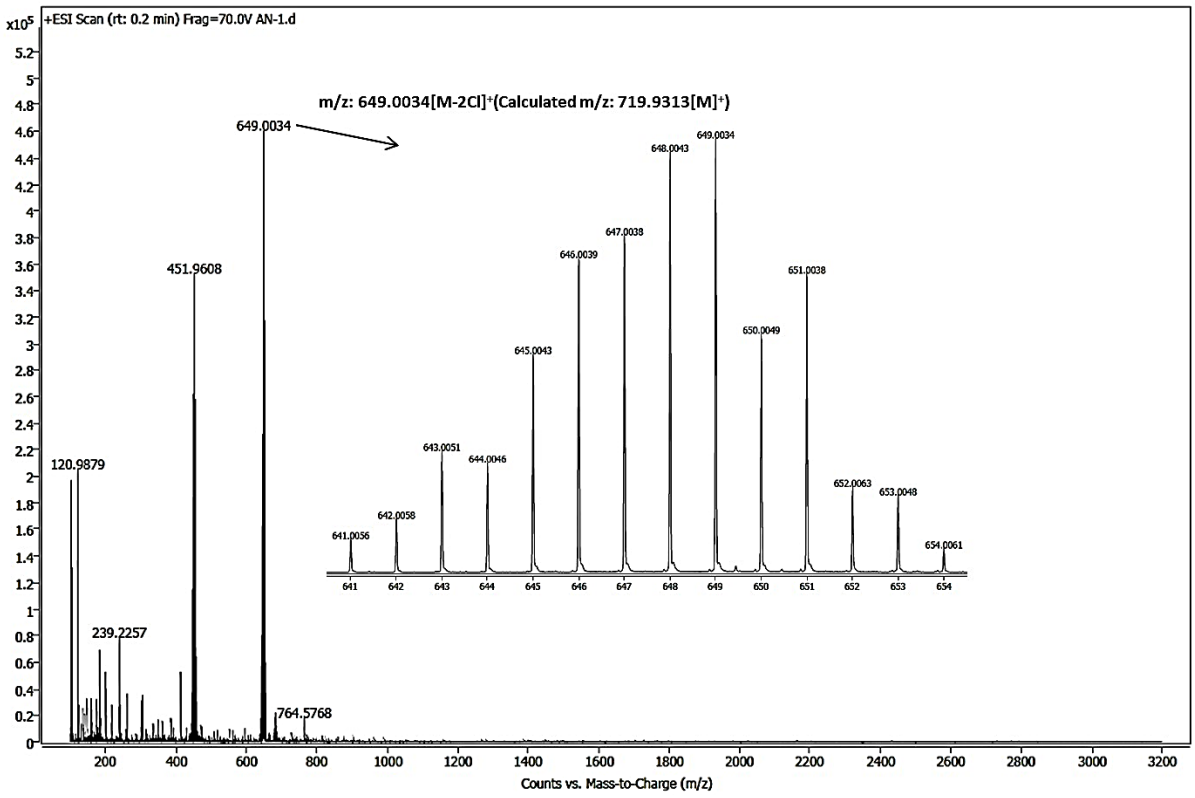

Figure S28. HR-MS spectrum of complex **1**in CH_3OH + CH_3CN
m/z: Calculated : 719.9313$[M]^+$; Observed: 649.0034 $[M-2Cl]^+$

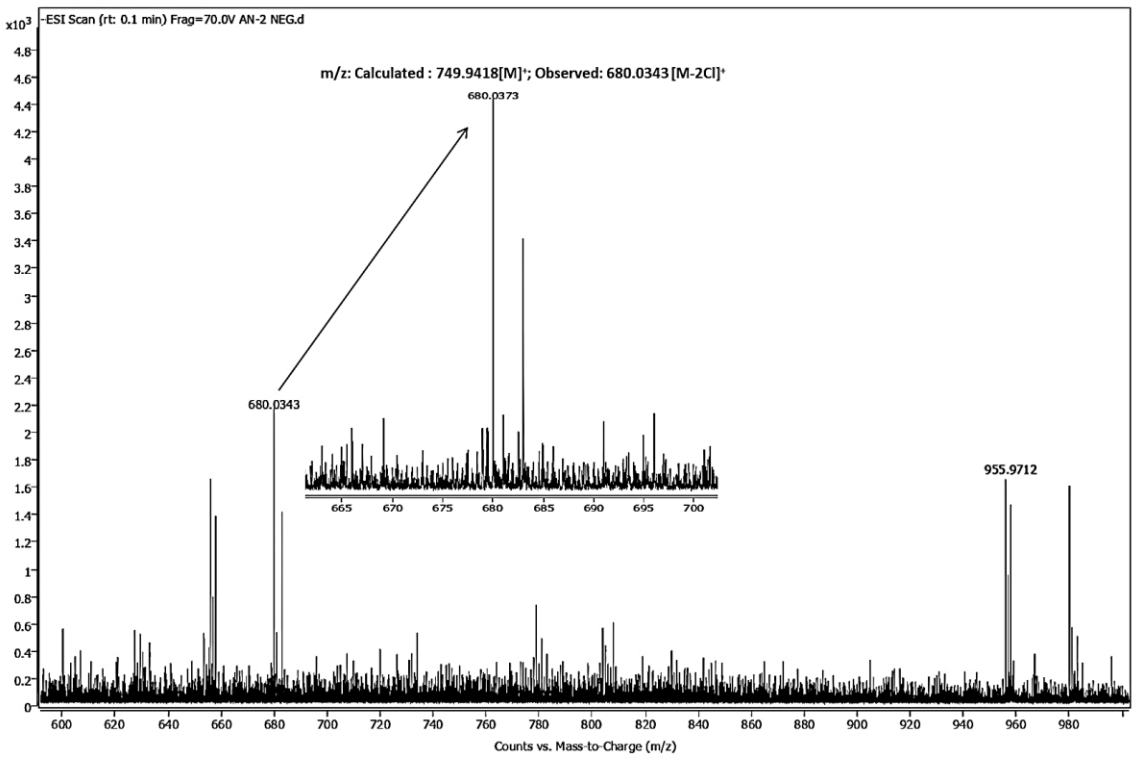

Figure S29. HR-MS spectrum of complex **2** in CH_3OH + CH_3CN
m/z: Calculated : 749.9418$[M]^+$; Observed: 680.0343 $[M-2Cl]^+$

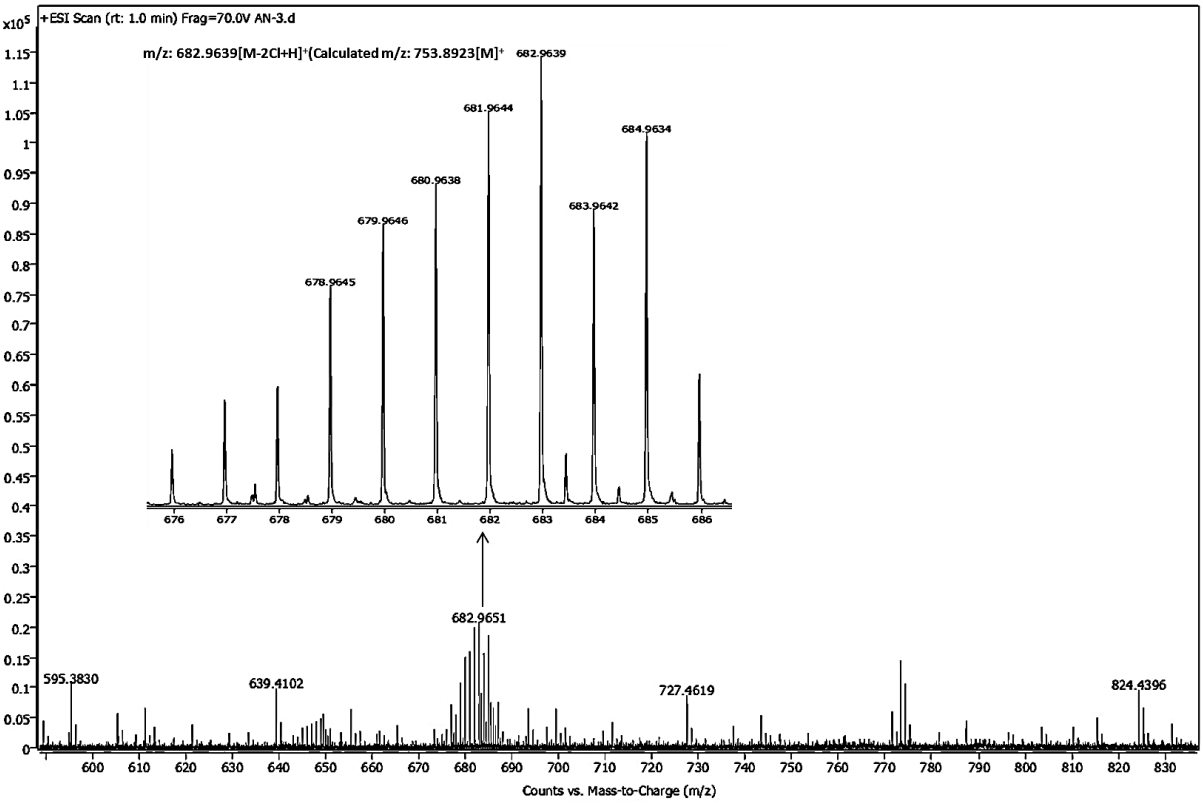

Figure S30. HR-MS spectrum of complex **3** in CH_3OH + CH_3CN
m/z: Calculated : 753.8923$[M]^+$; Observed: 682.9639 $[M-2Cl-H]^+$

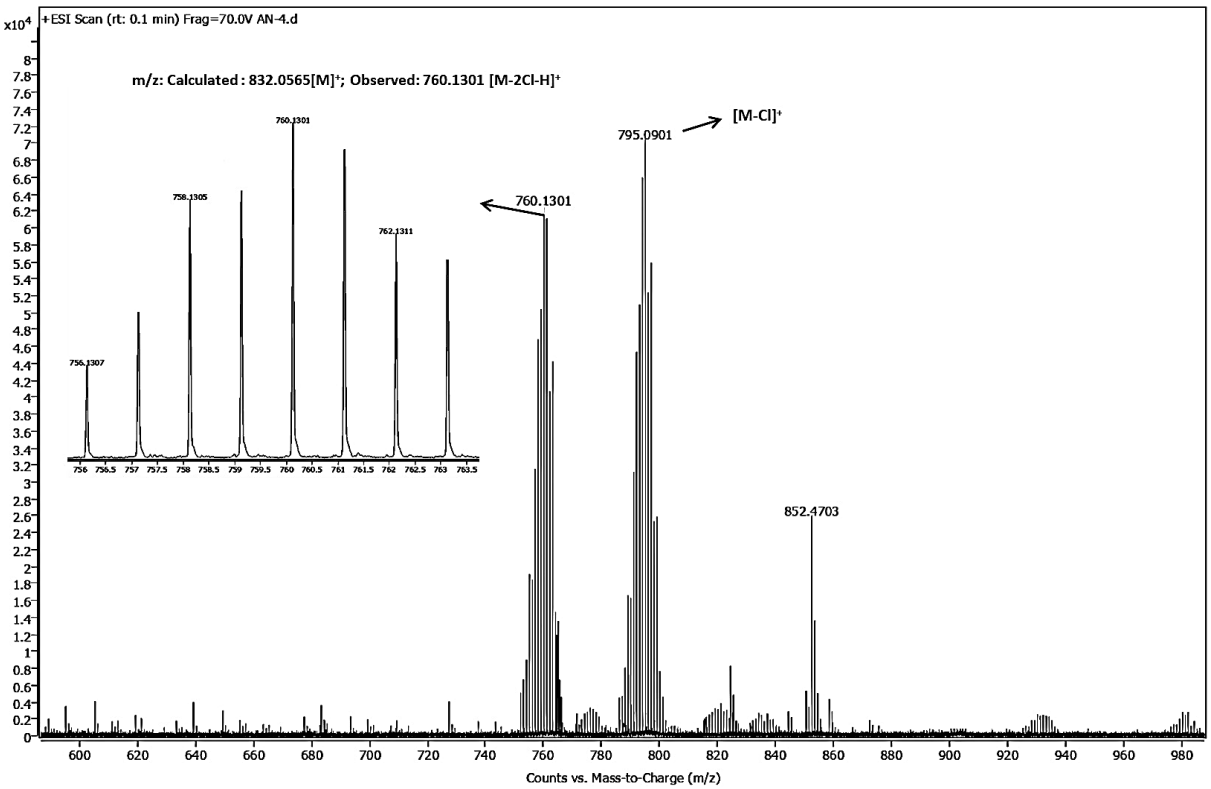

Figure S31. HR-MS spectrum of complex **4** in CH_3OH + CH_3CN
m/z: Calculated : 832.0565[M]+; Observed: 760.1301 [M-2Cl-H]+

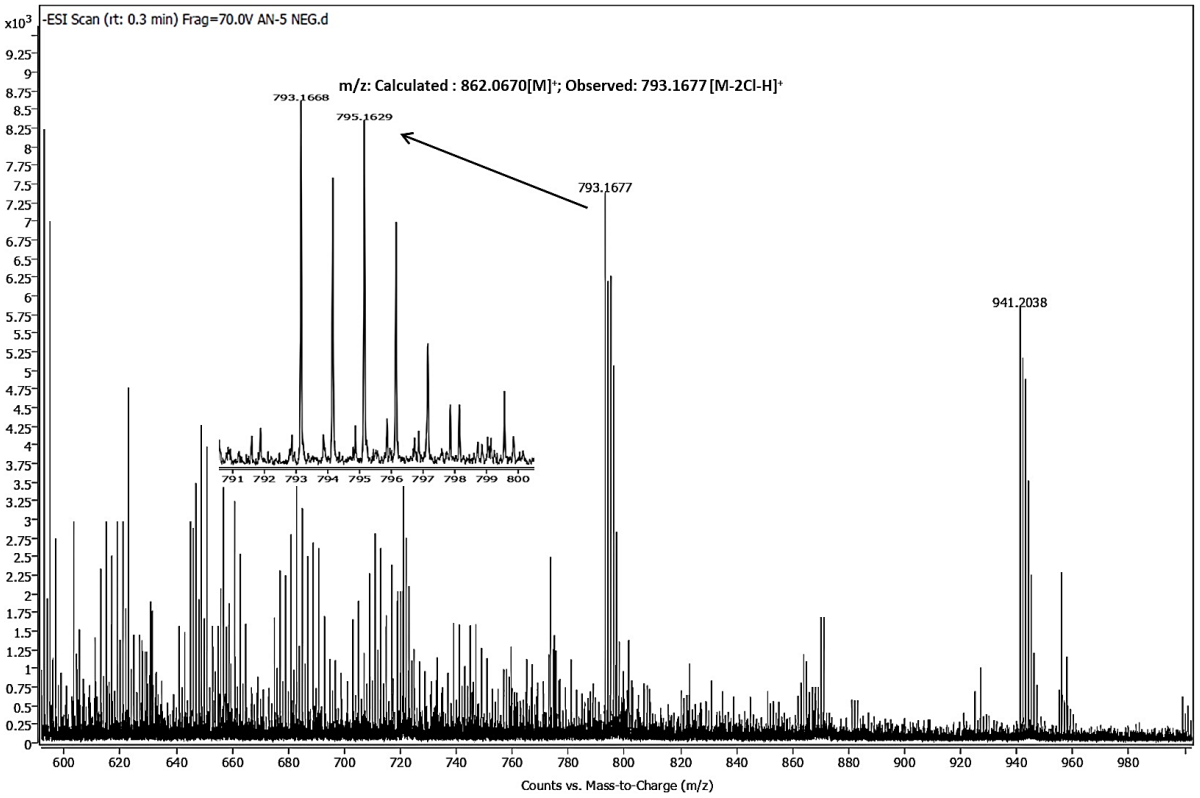

Figure S32. HR-MS spectrum of complex **5** in CH_3OH + CH_3CN
m/z: Calculated : 862.0670[M]+; Observed: 793.1677 [M-2Cl-H]+

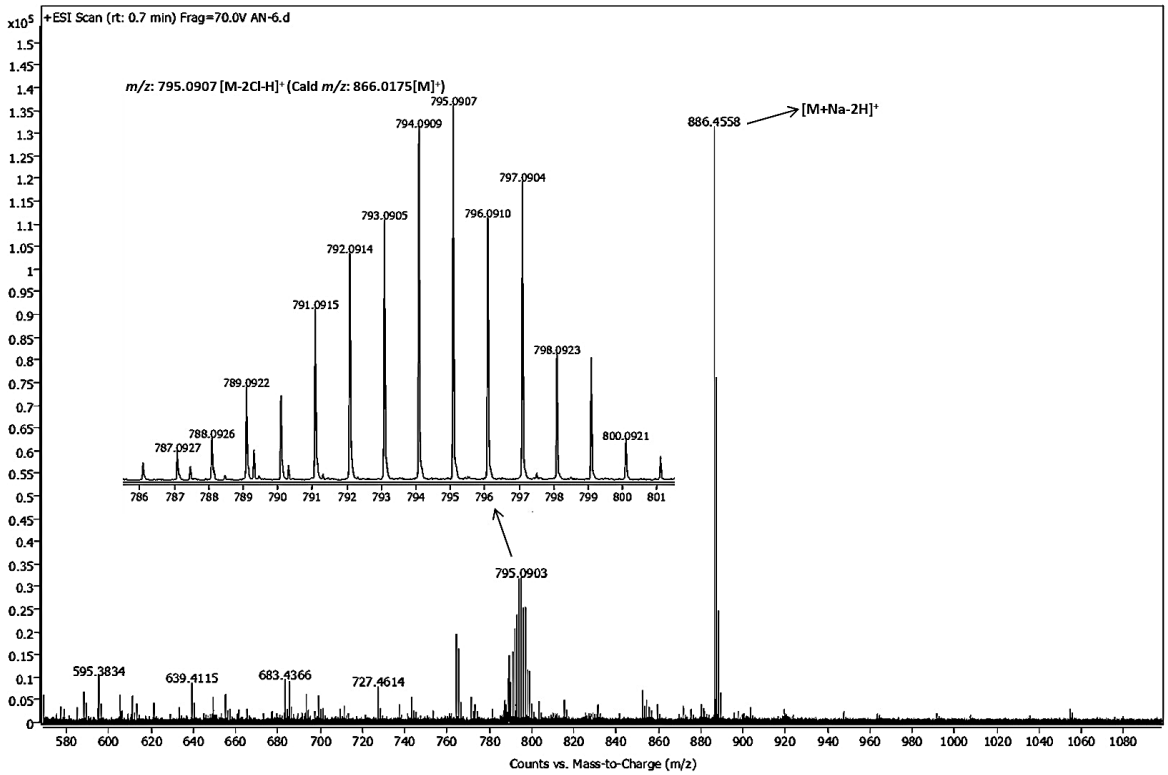

Figure S33. HR-MS spectrum of complex **6** in CH_3OH + CH_3CN
m/z: Calculated: 866.0175$[M]^+$; Observed: 795.0907 $[M\text{-}2Cl\text{-}H]^+$

8. Table S1: Crystal data and structure refinement for complex 1 and 6

Empirical formula	$C_{30}H_{24}Cl_2N_2O_2Ru_2$	$C_{38}H_{39}N_2O_2Cl_3Ru_2.CH_2Cl_2$
CCDC number	2262243	2262242
Formula weight	717.572	949.13
Temperature/K	293	295(2)
Crystal system	monoclinic	monoclinic
Space group	Pn	$P2_1/n$
a/Å	10.1560(7)	9.2299(3)
b/Å	12.8167(7)	23.8454(14)
c/Å	11.2086(6)	17.9871(7)
α/°	90	90
β/°	110.167(7)	93.269(3)
γ/°	90	90
Volume/Å^3	1369.55(15)	3952.3(3)
Z	2	4
ρ_{calc}g/cm^3	1.740	1.595
μ/mm^{-1}	1.329	1.138
F(000)	708.0	1912.0
Crystal size/mm^3	0.26 × 0.21 × 0.03	0.26 × 0.12 × 0.04
Radiation	Mo Kα (λ = 0.71073)	Mo Kα (λ = 0.71073)
2Θ range for data collection/°	6.68 to 58.82	6.734 to 58.814
Index ranges	-13 ≤ h ≤ 13, -17 ≤ k ≤ 12, -15 ≤ l ≤ 11	-10 ≤ h ≤ 12, -23 ≤ k ≤ 31, -23 ≤ l ≤ 18
Reflections collected	7204	20949
Independent reflections	4572 [R_{int} = 0.0314, R_{sigma} = 0.0513]	9263 [R_{int} = 0.0385, R_{sigma} = 0.0589]
Data/restraints/parameters	4572/2/343	9263/0/468
Goodness-of-fit on F^2	1.114	1.060
Final R indexes [I>=2σ (I)]	R_1 = 0.0379, wR_2 = 0.0689	R_1 = 0.0611, wR_2 = 0.1208
Final R indexes [all data]	R_1 = 0.0619, wR_2 = 0.0839	R_1 = 0.1066, wR_2 = 0.1433
Largest diff. peak/hole / e Å^{-3}	0.69/-0.52	1.04/-0.85

9. Table S2: Selected bond lengths(Å) and angles(°) for the complex 1 and 6

Bond lengths(Å)		
	Complex 1	**Complex 6**
Ru1-Cl1	2.383(2)	2.4135(17)
Ru1-O1	2.074(5)	2.059(4)
Ru1-N2	2.092(5)	2.089(4)
Ru1-C19	2.110(10)	2.218(6)
Ru1-C20	2.178(11)	2.196(5)
Ru2-C29	2.166(9)	2.221(7)
Ru2-C30	2.169(9)	2.180(6)
O1-C1	1.255(8)	1.285(6)
N1-N2	1.438(5)	1.428(6)
N1-C1	1.335(10)	1.299(6)
C2-C3	1.402(11)	1.385(9)
Ru2-Cl2	2.418(4)	2.418(2)
*$Centroid_{Ru1\text{-}arene}$	1.645	1.662
*$Centroid_{Ru2\text{-}arene}$	1.663	1.662

Bond angles(°)		
	Complex 1	**Complex 6**
O1-Ru1-Cl1	84.71(16)	85.15(13)
O1-Ru1-N2	76.7(2)	75.97(14)
O1-Ru1-C19	146.9(4)	150.29(19)
O1-Ru1-C20	163.0(4)	113.4(2)
O1-Ru1-C21	148.9(4)	90.0(2)
O1-Ru1-C22	111.8(4)	93.4(2)
O1-Ru1-C23	91.8(3)	123.2(2)
O1-Ru1-C24	97.6(4)	160.8(2)
N2-Ru1-Cl1	85.99(18)	85.33(13)
N2-Ru1-C19	92.8(3)	133.3(2)
N2-Ru1-C20	103.6(3)	170.5(2)
N2-Ru1-C21	134.1(4)	146.2(2)
N2-Ru1-C22	170.7(3)	110.6(2)
N1-Ru2-Cl2	84.19(17)	85.25(14)
N1-Ru2-C29	152.1(4)	132.8(2)
C29-Ru2-Cl2	87.2(3)	92.3(3)
C30-Ru2-Cl2	106.2(3)	115.7(3)
C1-O1-Ru1	114.2(5)	114.9(3)
N2-N1-Ru2	114.3(3)	113.7(3)
C1-N1- N2	111.0(5)	112.2(4)

Table S3. Hydrogen bonds in crystal of complexes **1** and **6**. Distances are in [Å] and angles are in [°].

D-H···A	d(D–H)	d(H···A)	d(D···A)	<(DHA)
		Complex 1		
C(14)—H(14)•••Cl(1)#1	0.93	2.81	3.6210(2)	146.0
C(23)—H(23)•••Cl(2)#2	0.93	2.82	3.6616(3)	152.0
		Complex 6		
C(23)—H(23)•••Cl(3)#3	0.93	2.72	3.5803(2)	154.0
C(24)—H(24)•••O(1)#3	0.93	2.33	3.1952(2)	155.0
C(31)—H(31)•••O(2)#4	0.93	2.33	3.1680(2)	150.0
C(32)—H(32)•••Cl(1)#4	0.93	2.77	3.6584(2)	161.0

Symmetry operators used to generate equivalent atoms:
#1: 1/2+x,1-y,-1/2+z; #2: 1/2+x,2-y,1/2+z; #3: 1+x,y,z; #4: -1+x,y,z

Table S4. Geometrical parameters of C—H•••Cg(J)(π-ring) interactions for complexes **1** and **6**.

C-H(I)•••Cg(J)	H(I)•••Cg(J) [Å]	H-Perp [Å]	γ [°]	C-H(I)•••Cg(J) [°]
Cg(1): C(2)-C(7); Cg(2): C(9)-C(13)-C(18) **Complex 1**				
C(21)-H(21)•••Cg(2)[1]	3.5073(2)	5.0045	-2.74	138
Complex 6				
C(20)-H(20)•••Cg(1)	3.3945(2)	5.6993	2.61	138
C(35)-H(35)•••Cg(2)	3.7783(17)	6.6031	-2.72	139

γ = angle H(I)→Cg(J) vector and normal to plane J.
Symmetry codes: 1: 1/2+x,1-y,1/2+z

10. Stability Studies

Chemical stability in aqueous media or physiological conditions is essential for advancing drugs toward clinical development. Hence, the stability of synthesized complexes (**1-6**) has been investigated by UV-vis spectra in a 1:9 (v/v) DMSO/phosphate buffer at a pH of 7.4. The electronic spectral pattern of complexes (**1-6**) has been monitored at varied time intervals. When the duration was extended to 72 hours, all the spectral peaks expressed a marginal reduction in absorbance intensities without changing the overall spectral pattern. The observed hypochromic shift clearly indicates the replacement of chloride by water in an aqueous medium. The significant findings of this investigation showed that all of the synthesized complexes (**1-6**) are stable in an aqueous medium and suitable for further biological studies (Figure S34-S39). The outcomes are concomitant with previously reported arene ruthenium complexes with labile chloride ligands.[8]

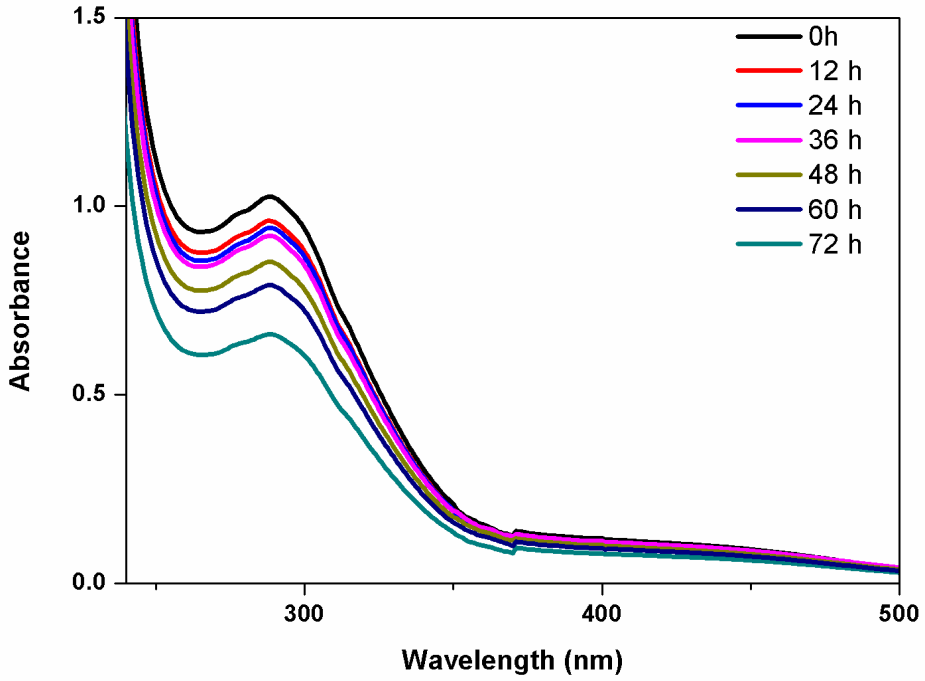

Figure S34. Stability study for Complex**1**

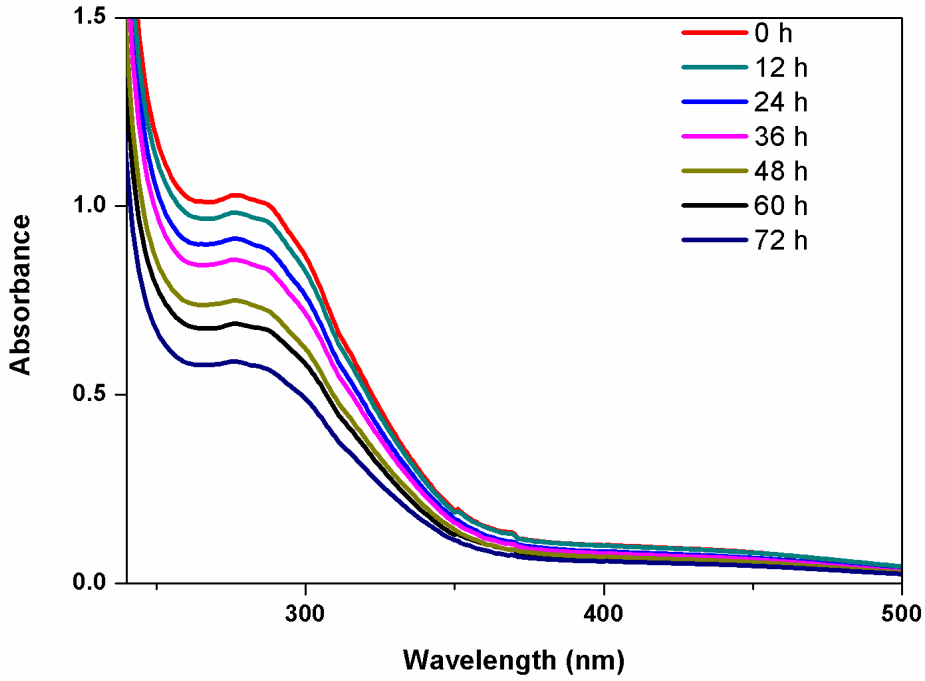

Figure S35. Stability study for Complex**2**

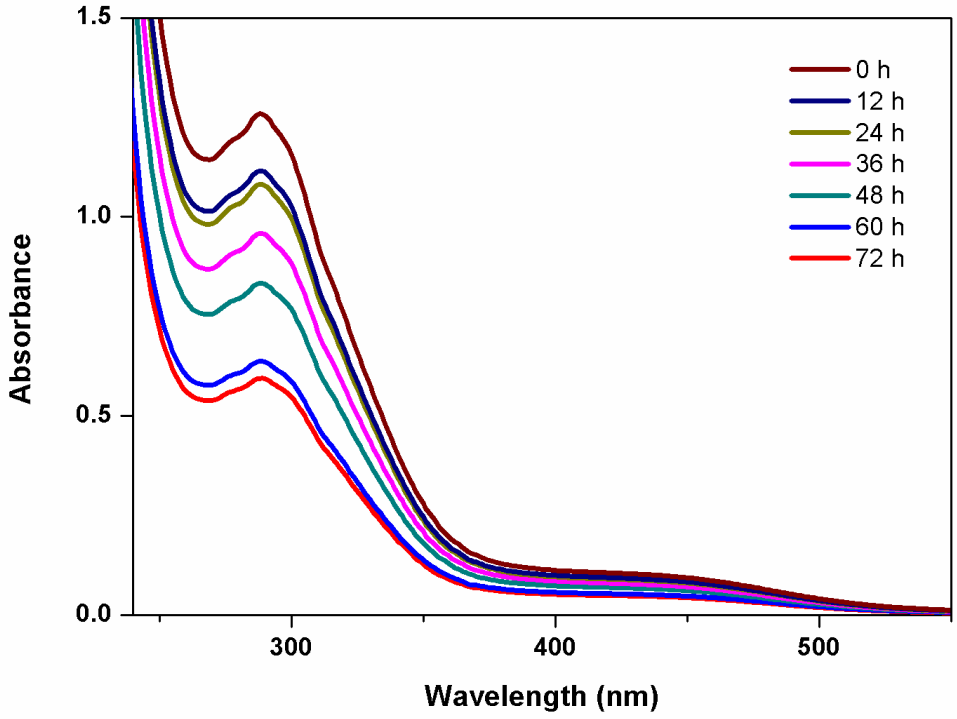

Figure S36. Stability study for Complex **3**

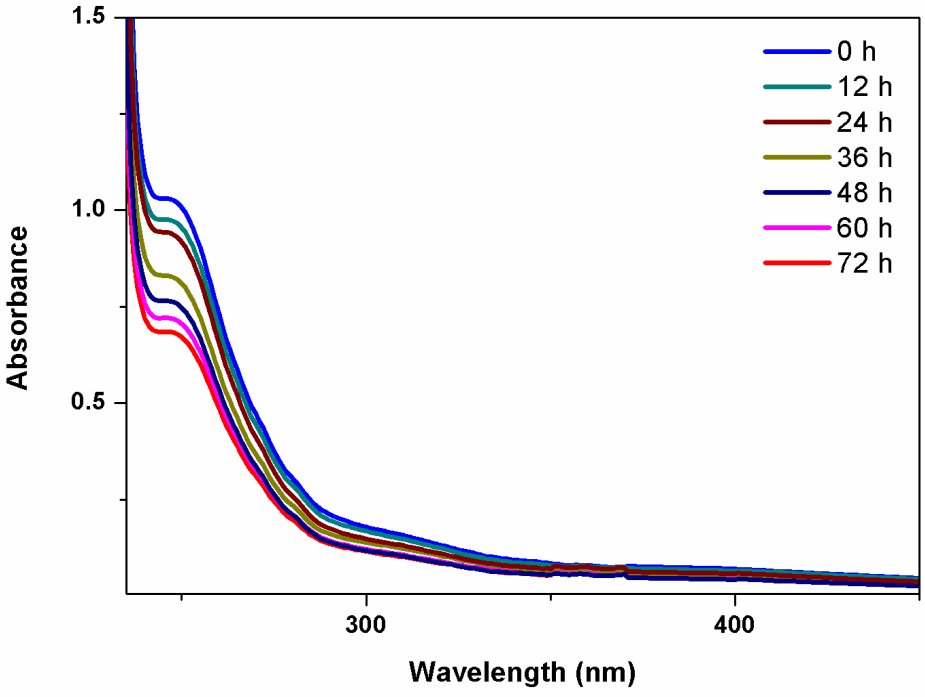

Figure S37. Stability study for Complex **4**

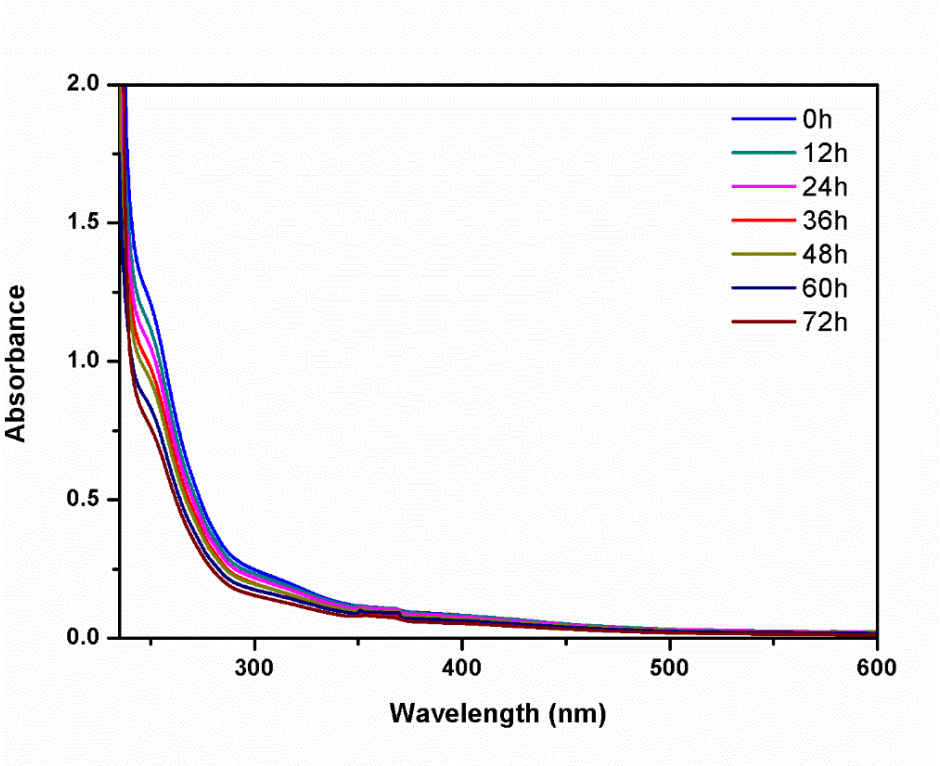

Figure S38. Stability study for Complex **5**

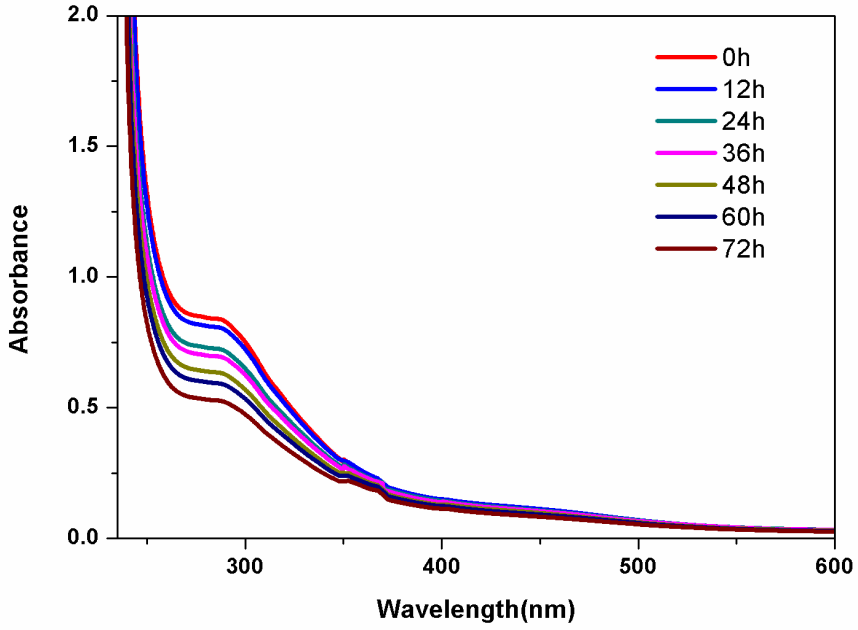

Figure S39. Stability study for Complex **6**

11. Partition Coefficient Determination (LOG P)

Lipophilicity or partition coefficient, is crucial in the cellular absorption of compounds *via* passive diffusion. It implies the equilibrium of water and a lipid-like organic solvent, such as n-octanol. The proportion of concentrations in the two phases is represented by log P (log P = [drug](in octanol)/[drug](in water)). When log P is positive, the complex has an affinity for the lipid phase; when it is negative, the complex has a stronger attraction to water. By utilizing the n-octanol/water system, log P values were computed for each of the titled complexes (**1-6**). The corresponding estimated log P values for the complexes (**1-6**) are 1.27±0.12, 1.79±0.24, 1.54±0.27, 1.68±0.14, 2.04±0.09 and 1.83±0.18 (Figure S40). It has been noted that the lipophilicity is likely to differ among the complexes which might be due to the variation in the different arene moieties and the nature of the substituent in the ligands. Further, complexes (**4-6**) exhibit greater lipophilicity than complexes (**1-3**) due to the presence of *p*-cymene moiety and electron-releasing methoxy substituent. Therefore, the complexes with higher lipophilicity can penetrate into the cancer cells via passive diffusion and are further illustrated by the MTT assay.[9]

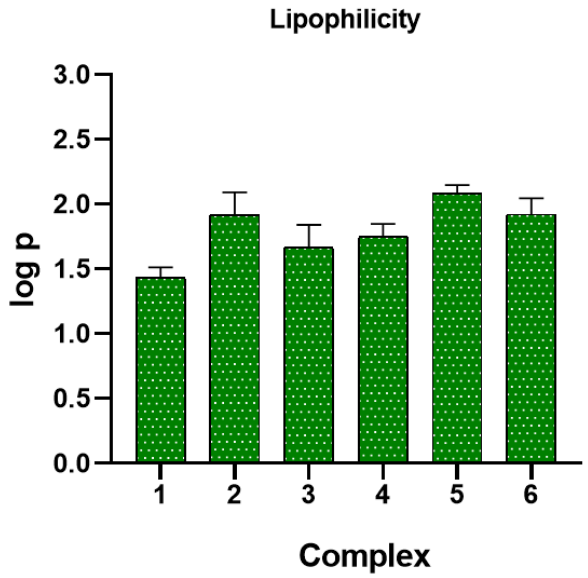

Figure S40. Lipophilic behaviour of complexes (**1–6**) in n-octanol/water system

12. Table S5. Cytotoxicity of complexes (**1-6**) and cisplatin against distinct breast cancer cells and non-cancerous HEK-293 cells.

IC_{50} ± SD (μM)					
Compound	**MCF-7**	**SkBr3**	**MDA-MB-468**	**MDA-MB 231**	**HEK-293**
NL1	>50	>50	>50	>50	>100
NL2	>50	>50	>50	>50	>100
NL3	>50	>50	>50	>50	>100
$Ru^{II}(\eta^6$-benzene) precursor	>100	>100	>100	>100	>100
$Ru^{II}(\eta^6$-*p*-cymene) precursor	>100	>100	>100	>100	>100
1	10.8±0.9 (24.18)*	13.2±0.7 (20.06)*	25.2±0.2 (10.08)*	18.4±0.5 (14.4)*	261.1±0.2
2	7.1±0.7 (39.82)*	4.5±0.6 (63.18)*	20.1±0.4 (13.93)*	15.7±0.4 (18.62)*	284.3±0.5
3	9.4±0.4 (28.43)*	8.4±1.1 (31.31)*	22.7±0.7 (12.08)*	16.3±0.9 (15.90)*	269.3±0.6
4	9.5±0.8 (28.49)*	6.2±0.3 (42.56)*	19.2±0.2 (14.04)*	13.1±0.7 (20.03)*	272.4±0.6
5	5.8±0.3 (50.55)*	3.1±0.5 (93.67)*	15.8±0.1 (18.7)*	10.1±0.6 (27.37)*	293.9±0.8
6	6.2±0.8 (46.28)*	5.5±0.2 (51.80)*	16.2±.9 (17.18)*	11.8±0.7 (25.22)*	286.5±0.2
Cisplatin	13.2±0.7 (7.11)*	10.8±0.7 (9.33)*	13.3±0.1 (6.92)*	14.3±0.4 (6.64)*	95.2 ±0.3

[a]Incubation time: 48 h; Data expressed in terms of mean IC_{50} (μM) ± SD; SkBr3 (HER2 positive) breast cancer cells,MCF-7(Metastatic breast cancer cells);MDA-MB-468 and MDA-MB-231(triple negative)breast cancer cells and HEK-293 (normal kidney)cells. *Selectivity Index(SI)

13. References

1. M. A. Bennett and A. K. Smith, *Dalton Trans.,*1974, **2**, 233-241..

2. M. A. Bennett, T. N. Huang, T. W. Matheson, A. K. Smith, S. Ittel and W. Nickerson, *Inorg. Synth*. 1982, 74.

3. I. Vogel, *Text Book of Practical Organic Chemistry*, fifth ed., Longman, London, **1989**.

4. G. M. Sheldrick, *Acta Crystallogr. A*, 2008, **64**, 112-122.

5. L. J. Farrugia, *J. Appl. Crystallogr.* 1997, **30**, 565-565.

6. F. Wang, H. Chen, S.Parsons, I. D. H. Oswald, J. E. Davidson and P. J. Sadler, *Chem. Eur. J.* 2003, **9** , 5810-5820.

7.(a) R. K. Gupta, G. Sharma, R. Pandey, A. Kumar, B. Koch, P. Z. Li and D. S. Pandey,

Inorg. chem., 2013, **52**, 13984-13996. (b) R. K. Gupta, R. Pandey, G. Sharma, R. Prasad, B. Koch, S. Srikrishna and D. S. Pandey, *Inorg. chem.,* 2013, **52**, 3687-3698.

8. (a) M. Li, L. Lai, Z. Zhao and T. Chen, *Chem. Asian J.,* 2016, **11**, 310-320. (b) H. Wang, N. J. Deyonker, H. Gao, L. Ji, C. Zhao and Z. Mao, *J. Organomet. Chem.,* 2012, **704**, 17–28. (c) F. Wang, H. Chen, S. Parsons, I. D. H. Oswald, J. E. Davidson and P. J. Sadler, *Chem. Eur. J.,*2003, **9**, 5810-5820.

9. (a) X. Liu, B. Testa and A. Fahr, *Pharm. Res.,* 2011**, 28**, 962-977. (b) H. Huang, P. Zhang, Y. Chen, L. Ji and H. Chao, *Dalton Trans.,* 2015, **44**, 15602-15610. (c) S. H. Van Rijt, A. Mukherjee, A. M. Pizarro and P. J. Sadler, *J. Med. Chem.,* 2010, **53**, 840-849.